Catarina Boloto Barbosa

BsC Biochemistry

Exploring respiratory enzymes from *Staphylococcus aureus*

Dissertation for obtaining a Master Degree in
Biochemistry for Health

Supervisor: Manuela Pereira, Ph.D, ITQB-NOVA

Co-supervisor: Patrícia Refojo, Ph.D, ITQB-NOVA

October 2018

Catarina Boloto Barbosa

BsC Biochemistry

Exploring respiratory enzymes from *Staphylococcus aureus*

Dissertation for obtaining a Master Degree in
Biochemistry for Health

Supervisor: Manuela Pereira, Ph.D, ITQB-NOVA

Co-supervisor: Patrícia Refojo, Ph.D, ITQB-NOVA

Jury:

President: Pedro Matias, Ph.D, ITQB-NOVA
Opponent: Federico Herrera, Ph.D, ITQB-NOVA
Members of jury: Margarida Archer, Ph.D, ITQB-NOVA

Instituto de Tecnologia Química e Biologica António Xavier Universidade Nova de Lisboa

October 2018

Copyright

Agradecimentos

Em primeiro gostaria de agradecer ao ITQB por ter tornado esta tese possível e agradecer a todos os seus colaboradores que de alguma forma ajudaram na realização da mesma. De seguida gostaria de agradecer à minha orientadora Dra. Manuela Pereira e à minha coorientadora Dra. Patrícia Refojo, por terem-me aceite para este projeto e ajudarem-me ao longo deste caminho. Ao longo deste ano que passou não só me ajudaram a crescer e a desenvolver capacidades científicas como também ensinaram-me tanto. Também gostaria de agradecer ao Professor Miguel Teixeira como responsável da *Metalloproteins and Bioenergetics Unit.*

Gostaria de agradecer aos meus colegas do laboratório *Biological Energy Transduction*: Filipe Sousa, Filipa Sena e Filipa Calisto. À Filipa Calisto gostaria de deixar um agradecimento muito especial, por todas as horas que me tiveste que aturar, por toda a amizade que me destes, Obrigada, pela ajuda, pelo apoio e pelas horas do chocolate, por tudo basicamente. Gostava também de agradecer ao Filipe Folgosa e à Maria Martins do grupo *Metalloenzymes and Molecular Bioenergetics*, pelo apoio, preocupação e carinho.

Neste longo ano conheci várias pessoas cuja sua paixão pela ciência inspiram-me e contagiaram, especialmente gostava de agradecer ao Paulo Castro por ter-me aturado e mesmo assim ser um amor de pessoa que me ajudava quando necessitava, à Sónia Pereira por todo o carinho partilhado e preocupação . À Helena Veiga queria agradecer a atenção, a preocupação e a ajuda que me deu.

Ao CERMAX e à Mass Spec Facility UniMS pela ajuda ao realizar esta tese.

Quero agradecer à minha segunda família, uma vez que são o meu pilar de confiança e que se encontram sempre disponíveis para mim quando eu mais necessito. Por aturarem-me à imenso tempo (quase 5 anos) aos meus queridos fofos muito obrigada: Ricardo Barras, Miguel Bernardo, Diogo Carregosa, Sérgio Torres, Cláudia Freitas e Rúben Guerreiro, um obrigado cheio de carinho.

À minha família que desde sempre me apoiou, por todo o carinho dado, apesar de o pouco tempo que conseguia ir a casa, muito obrigada.

Ricardo Barras, a ti eu quero agradecer os conselhos, o apoio, as palavras de confiança, a força para conseguir enfrentar este longo ano, pelos longos passeios para esvaziar a cabeça, muito muito obrigada, por todo o que escrevi e o que não consigo expressar por palavras. Por isso e tudo mais Obrigada meu amor.

Resumo

Staphylococcus aureus é um agente patogénico oportunista que pode causar doenças com diferentes manifestações, o que em parte se deve à rápida capacidade adaptativa do organismo. Muitos aspetos do **metabolismo energético** e da **cadeia respiratória** ainda são pouco entendidos. Neste trabalho estudaram-se três enzimas da cadeia respiratória: o **sistema gerador de potencial de membrana** (Mps**AB)** e duas **malato:quinona oxidorreductases** (MQO).

A enzima MpsAB é proposta estar envolvida no processo de conservação de energia em *S. aureus* devido à homologia entre a sequência da subunidade MpsA com a subunidade NuoL do complexo I de *Escherichia coli* que se hipotetiza ser responsável por translocar protões. Testes de expressão heterológa do complexo e otimizção do processo de purificação foram feitos com o intuito de se obter uma boa preparação para subsequentes estudos bioquímicos e assim se aprofundar o conhecimento sobre o complexo.

As MQOs são proteínas monótopicas que catalisam a oxidação do malato a oxaloacetato com a simultânea redução de quinona a quinol. *S. aureus* possui dois genes anotados de MQO, *mqoI* e *mqoII*. Para compreender mais sobre as implicações metabólicas das duas MQOs foi estudado o crescimento da bactéria em diferentes fontes de carbono (glucose, lactato ou acetato). Foram estudadas três estirpes bacterianas; duas com transposões em cada um dos genes que codificam as MQOs e a estirpe selvagem (WT). Os padrões de excreção e assimilação dos nutrientes das estirpes em estudo foi analisado por **ressonância magnética nuclear**. A expressão heteróloga das MQOs foi realizada em *E. coli*. Para posterior análise bioquimica tentou-se otimizar a purificação das duas enzimas.

Com estes estudos demostramos que as MQOs são enzimas metabólicas importantes e que a nivel metabólico são diferentes entre si uma vez que apresentam diferentes padrões de excreção e assimilação. Os mutantes apresentaram um crescimento reduzido em comparação com o WT. Isto demostra a importância metabólica das duas enzimas, o que as torna possíveis alvos terapêuticos para o futuro.

Palavras-Chave: Metabolismo Energético; Cadeia Respiratória; Sistema gerador de potencial de membrana AB ; Malato:quinona Oxidorreductases; Ressonância Magnética Nuclear

Abstract

Staphylococcus aureus is an opportunistic pathogen that can cause various disease patterns due to its high adaptative capacity. Many aspects of the **energy metabolism** and its **respiratory chain system** are still poorly understood. Herein, we report our study of three respiratory enzymes: **Membrane potential-generating system** (Mps**AB**) and two **malate:quinone oxidoreductases** (MQO).

The MpsAB enzyme is a membrane complex proposed to be involved in energy conservation in *S. aureus* due the sequence homology of the subunit MpsA with the proton-translocation subunit NuoL of complex I from *Escherichia coli*. To further investigate the complex a series of expression tests were made to achieve its heterologous expression in *E. coli*. We also tried to optimize protein purification for biochemical studies.

MQO is a membrane-associated protein that catalyses the oxidation of malate to oxaloacetate with simultaneous reduction of quinone to quinol. It is described that *S. aureus* encodes two MQO genes, *mqoI* and *mqoII*, though little is known about their differences. To understand the metabolic impact of these proteins in *S. aureus*, growths of wild-type (WT) strain and of strains containing transposons in the genes coding for both MQOs were performed, using different carbon sources: glucose, lactate or acetate. **Nuclear magnetic resonance** (NMR) was employed to analyse the uptake and secretion patterns of the three strains understudy when grown in glucose. Furthermore, the purification of these proteins was performed although only for MQOII preliminary biochemical studies were performed.

Herein we demonstrated that both MQOs are important metabolic enzymes since the mutants showed an impaired growth compared to the WT. Moreover, we can conclude that the enzymes are metabolically different, since the loss of one was not compensated by the other. By demonstrating that both enzymes are important for *S. aureus* metabolism, MQOs should be considered as drug targets candidates for the future.

Keywords: Energy Metabolism, Respiratory Chain, Membrane Potential-Generating System AB; Malate:quinone Oxidoreductases; Nuclear Magnetic Resonance

Index

Index of Figures

Index of Tables

Abbreviations

Amp	**Amp**icillin
CA-MRSA	**C**ommunity **A**ssociated **M**ethicillin-**R**esistant ***S****taphylococcus* ***a****ureus*
CDMA	**C**hemical **D**efine **M**edia supplemented with **A**cetate
CDMG	**C**hemical **D**efine **M**edia supplemented with **G**lucose
CDML	**C**hemical **D**efine **M**edia supplemented with **L**actate
CoA	**Co**enzyme **A**
DCPIP	2,6-**Di**chloro**p**henoll**i**ndo**p**henol
ddH$_2$O	**D**ouble **D**istilled **W**ater
DDM	*n*-**D**odecyl β-**D**-**M**altoside
DMN	2,3-**D**imethoxy-5-**M**ethyl-1,4-**N**aphthoquinone
dNTP	**D**eoxy**n**ucleotide Tri**p**hosphate
EDTA	**E**thylene**d**iamine**t**etraacetic **A**cid
Ery	**Ery**thromycin
ETCs	**E**lectron **T**ransport **C**hain (**S**ystem)
FAD	**F**lavin **A**denine **D**inucleotide
FMN	**F**lavin **M**ono**n**ucleotide
GFP	**G**reen **F**luorescent **P**rotein
HA-MRSA	**H**ospitals **A**ssociated **M**ethicillin-**R**esistant ***S****taphylococcus* ***a****ureus*
HEPES	4-(2-**H**ydroxy**e**thyl)-1-**P**iperazine**e**thane**s**ulfonic Acid
6xHisTag	Poly**his**tidine-Tag
HQNO	2-N-Heptyl-4-**H**ydroxy**q**uinoline **n**-**O**xide
iLDH	NAD-Independent Lactate Dehydrogenase
IMAC	**I**mmobilized **M**etal **I**on **A**ffinity **C**hromatography
IPTG	**I**so**p**ropyl-β-D-1-**T**hio**g**alactopyranoside
KPi	**P**hosphate buffer
LB	**L**uria Bertani **B**roth
LQO	Lactate:Quinone Oxidoreductase
MDH	NAD-Dependent L-Malate Dehydrogenase
Mps	**M**embrane **P**otential-Generating **S**ystem
MQO	Malate:Quinone Oxidoreductase
MRSA	**M**ethicillin **R**esistant ***S****taphylococcus* ***A****ureus*
MS	**M**ass **S**pectrometry
NAD	**N**icotinamide **A**denine **D**inucleotide
NDH-2	Type 2 NADH:Quinone Oxidoreductase
NMR	**N**uclear **M**agnetic **Resonance**

OD_{600nm}	**O**ptical **D**ensity At **600 nm**
PCR	**P**olymerase **C**hain **R**eaction
PMSF	**P**henyl**m**ethane**s**ulfonyl **F**luoride
RNAP	T7 **RNA P**olymerase
SDH	Succinate:Quinone Oxidoreductase
SDS-PAGE	**S**odium **D**odecyl **S**ulfate-**P**olyacrylamide **G**el **E**lectrophoresis
SOB	**S**uper-**O**ptimal **B**roth
SOC	**S**uper-**O**ptimal
TAE	**T**ris-**A**cetate- **E**thylenediaminetetraacetic Acid
TB	**T**errific **B**roth
TCA	**T**ri**c**arboxylic **A**cid
Tn	**T**ransposon **M**utants
Tris	**Tris**(Hydroxymethyl)Aminomethane
TSA	**T**ryptic **S**oy **A**gar
TSP	**T**rimethyl**s**ilyl**p**ropanoic Acid

1. State of Art

1.1 Energetic Metabolism

1.1.1 Energy and Life

All living organisms need energy to live, grow and reproduce. This is only possible due to their ability to harvest energy and convert it. So, it could be said that the ability to perform energy transduction is the essence of Life [1–3].

In 1961, Peter Mitchell postulated the Chemiosmotic Theory, which says that the energy extracted from a biological oxidation-reduction reaction is transduced in a transmembrane electrochemical potential [1,3,4]. The transmembrane electrochemical potential is a difference in proton concentration and a difference in electric potential across the membrane [4–6]. To synthesise adenosine triphosphate (ATP), cells can use the ATP synthases, which catalyze the reaction of ATP formation by dissipating the difference in proton concentration through the membrane [1–3].

1.1.2 Metabolism

Metabolism can be described as the set of chemical transformations that happen in a cell by successive enzymatic reactions [2,]. The metabolism of heterotroph organisms has two phases. A degradative phase, called catabolism, in which organic nutrient molecules, such as carbohydrates, fatty acids or proteins, are converted into simple and smaller products (e.g. lactic acid, carbon dioxide or ammonia). During this phase occurs energy release. The other phase is the biosynthesis phase, called anabolism, in which the simple precursors are transformed into larger and complex molecules (e.g. lipids, proteins, polysaccharides or nucleic acids). To perform this phase an input of energy is needed [1,2,7].

The cells need controlled regulation of the metabolism; those regulatory processes allow to maintain its steady state. When a perturbation of this state occurs, by external factors or energy supplies, the regulatory mechanism for each pathway is activated to achieve a new steady state [7].

Organisms can use carbohydrates as their primary source to obtain cellular energy. Glucose is a sugar with high potential energy [8], being a preferred carbon source for many bacteria, for instance *Escherichia coli*. It was observed that *E. coli* had a faster growth rate in the presence of glucose when compared with growths in the presence of other sugars [9].

There are two processes capable of producing energy from glucose: cellular respiration in which ATP production is due to the dissipation of membrane potential [10] and fermentation in which ATP is produced by substrate-level phosphorylation [2].

The cellular respiration involves three principal pathways: glucose oxidation; Krebs cycle, also known as Tricarboxylic Acid (TCA) cycle; and electron transport chains (system)-ETCs [2,3].

Glucose oxidation to pyruvic acid can be done by the glycolytic pathway producing two molecules of ATP and two reduced molecules of nicotinamide adenine dinucleotide (NADH). In eukaryotic and prokaryotic cells this process occurs in the cytoplasm [11]. Some organism, may use other pathways as the pentose phosphate pathway (which can occur simultaneously with glycolysis) that allows the oxidation of five carbon sugars as well as glucose oxidation to pyruvic acid [12]. Some bacteria can use the Entner-Doudoroff pathway that allows bacteria to metabolize glucose alternatively to the glycolysis or the pentose phosphate pathway [13]. Pyruvic acid is then transported to the mitochondrial matrix in the eukaryotic cell where it is converted to Acetyl coenzyme A (Acetyl-CoA). In prokaryotic cells this conversion occurs in the cytoplasm. The precursor Acetyl-CoA then enters the TCA cycle and it is metabolized by a series of oxidation reactions. During this pathway ATP is formed and two electron donors for the ECTs are produced, NADH and succinate. All the ATP is produced by substrate-level phosphorylation [2,3,11,14].

In the ETCs the reduced electron carries are oxidized and, in some of the complexes that compose the ETCs, proton translocation against the membrane potential also happens. This produces a membrane potential that is used by the last complex, the ATP synthase, to generate ATP by oxidative phosphorylation. In eukaryotic cells this happens in the inner membrane of the mitochondria whereas in prokaryotes this occurs in the inner part of the cell membrane [1,3,5,10,11].

To summarize, cellular respiration (Figure 1.1) is a process involved in ATP generation through membrane potential. Depending on the final acceptor it can be either aerobic, in the case of oxygen as final acceptor on the ETCs, or anaerobic if its final acceptor is a molecule other than O_2 [2,3,10,11]. For instance, nitrate ions (*Bacillus* [15] or *Pseudomonas* [16]) or sulphate (*Desulfovibrio* [17]) .

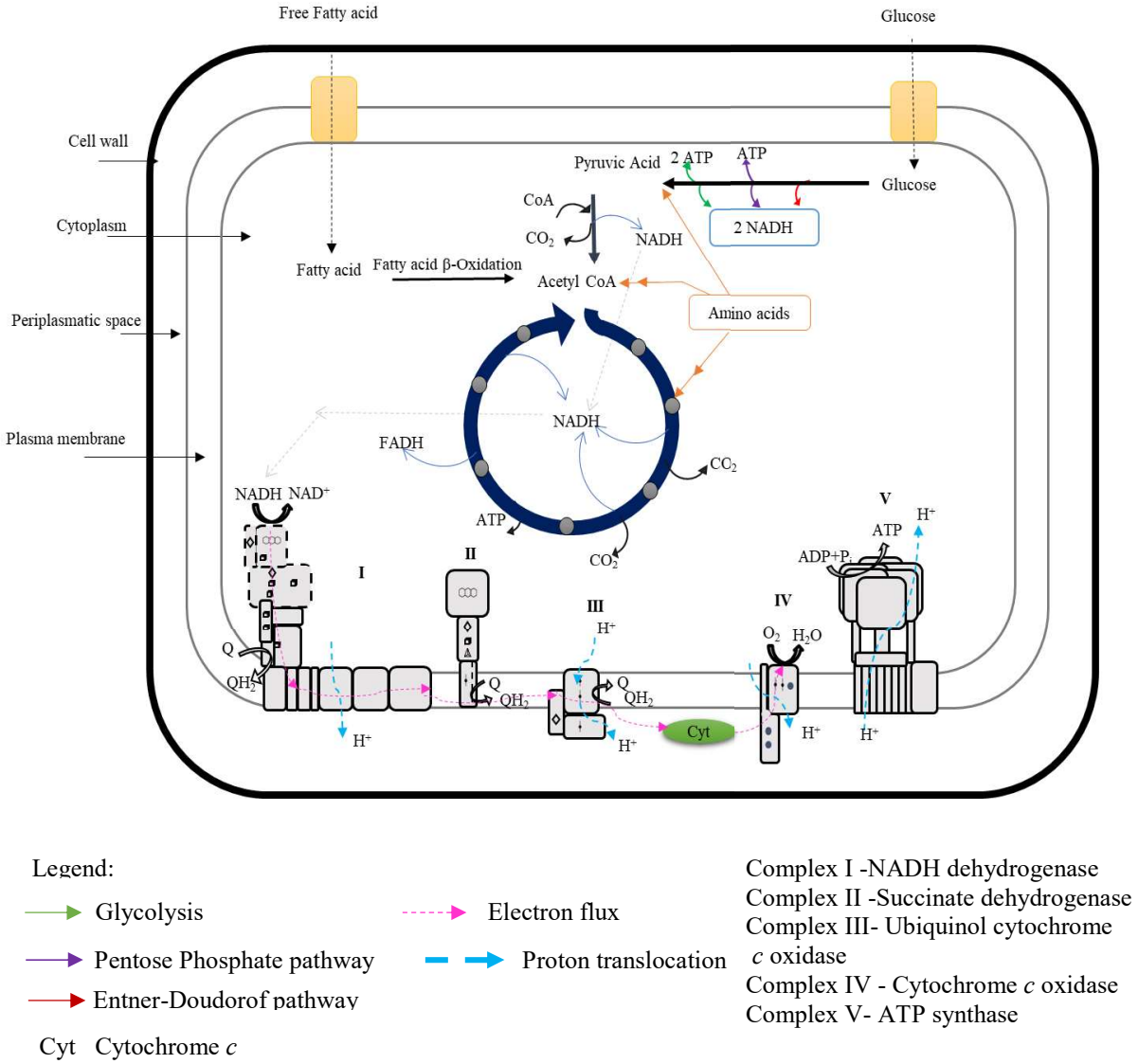

Figure 1.1-**Aerobic respiration**. Schematic representation of the aerobic respiration main phases. Fatty acid transporters and glucose transporters are present as yellow squares. Aerobic respiration has three phases: in the first glucose is converted to pyruvic acid with production of ATP and reduction of NADH. This conversion can be done by glycolysis or by alternative pathways such the pentose pathway or the Enter-Doudoroff pathway. Then, in the second phase, the Krebs cycle takes place where is observed the reduction of energy carriers, such as NADH, and production of succinate. These energy carries are then used in the third phase, the electron transport chain (system) where the electron transport and the ATP production occur. Here is also represented how the principal precursors of the aerobic respiration may be obtain by alternative ways. Double arrows indicate successive reactions. Adapted from Marreiros et.*al* [1] and Lehninger Principles of Biochemistry [2].

1.1.3 Respiratory chains

Respiratory chains are diverse, and this diversification is a consequence of the organisms metabolic needs [1,3]. Its composition commonly involves several protein complexes able to perform oxidation-reduction reactions. Some of these oxidoreductases are also capable of translocating protons across the membrane against the electrochemical gradient. In prokaryotes, these protein complexes are localized in the inner plasma membrane while in eukaryotes they are in the inner mitochondrial membrane. So, in the first, the translocation of protons is from cytoplasmic to periplasmic space and in the second it is done from mitochondrial matrix to the inter-membrane space [2,7].

The mammalian electron transfer chain is one of the best characterized metabolic pathway. It is composed of four complexes (I, II, III and IV) and mobile electron carriers, ubiquinone and cytochrome *c* (cyt *c*) that are responsible for electrons transfer between complexes [3,18].

Complex I – NADH:ubiquinone oxidoreductase- is an electron entry point in the ECTs and has approximately 1 MDa and 44 subunits [19,20]. Complex I uses the energy released in the NADH:quinone oxidoreduction, performed at the peripheral arm of the complex, to translocate ions across the membrane, which takes place in the membrane domain [21,22]. Complex II, named succinate:quinone oxidoreductase, catalyzes the oxidation of succinate to fumarate with the reduction of ubiquinone to ubiquinol. This complex does not perform ion translocation [23]. Electrons are transferred from ubiquinol to cytochrome *c* by Complex III (ubiquinol:cytochrome *c* oxidoreductase) in a reaction coupled with energy conservation [24,25]. The reduced cytochrome *c* then donates electrons to complex IV (cytochrome *c* oxidase), which is responsible for the reduction of molecular oxygen to water. Complex IV also translocate protons across the membrane [23].

1.1.4 Malate: Quinone Oxidoreductase

L-malate:quinone oxidoreductase (MQO) is a membrane-associated protein that catalyzes the oxidation of malate to oxaloacetate [1,26–31], a reaction that occurs in the TCA cycle. This enzyme is different from the well-studied cytoplasmic malate dehydrogenase (MDH) since it does not use NAD^+ as electron acceptor [31]. This protein is a monotopic enzyme, stabilized at the surface of the lipid bilayer by electrostatic or hydrophobic interactions. MQO contains flavin adenine dinucleotide (FAD) as a prosthetic group. FAD has a characteristic UV-visible spectrum with a maximum peak at 450 nm [31–33]. MQO transfers two electrons from *L*-malate to an oxidized FAD, producing oxaloacetate and a reduced FADH. Afterwards the electrons from FADH are transferred to an oxidized quinone leading to its reduction and FAD regeneration. *In vitro* the activity of detergent-solubilized MQO can be measured following the reduction of an artificial acceptor. Almost all the MQO's described to date are easily released from the membrane by low detergents concentration [28-32]. In *E. coli, Mycobacterium smegmatis* and *Mycobacterium phlei* it was observed that MQO activity was stimulated by FAD and lipids or detergent addition [31–33].

MQO has been reported in several Gram-positive and Gram-negative bacteria, like in *E. coli* [27], *Helicobacter pylori* [34], *Bacillus* [28], *Corynebacterium glutamicum* [31,35], *Pseudomonas aeruginosa*[30], *Pseudomonas ovalis*[36] and *Mycobacterium smegmatis*[37]. In some organisms, such as *M. smegmatis* [37] and *P. ovalis* [36], the MDH could not be detected, whereas in the others organisms both enzymes (MQO and MDH) were detected [35–40].

A variety of important human pathogens, *e.g.*, *H. pylori* [34], *Bacillus* [28], *C. glutamicum* [31] or *Plasmodium falciparum* [26], have genes encoding MQO's and these enzymes could be used as new drug therapy targets since mammalian cells have a soluble MDH that is present in the mitochondrial matrix with no homology with MQO [26].

1.1.5 Lactate: Quinone Oxidoreductase

Lactate:quinone oxidoreductases (LQOs) are membrane-associated enzymes that belong to the NAD^+-independent dehydrogenases family (enzymes reviewed by Garvie [41] in 1980 and more recently by Jiang *et.al* [42] in 2014). This enzyme catalyses the reduction of lactate to pyruvate using quinones as electron acceptors. LQO can be differentiated in *L*-LQOs or *D*-LQOs, depending on the chiral form of lactate used as substrates, either *L*-lactate or *D*-lactate, respectively [41].

The *L*-LQO enzymes, described to date have a FMN [43,44] as cofactor, or in the case of *Pseudomonas stutzeri A1501* [45] an iron-sulfur cluster, whereas *D*-LQO proteins have a FAD as cofactor [46–48].

1.2 *Staphylococcus aureus*

1.2.1 Brief overview and general characteristics

The Scottish surgeon, Alexander Ogston, isolated for the first-time *staphylococci* from human pus in 1880. The name *Staphylococcus* is the junction of the words *staphyle* (a bunch of grapes) and *kokkos* (berry) because when viewed at the microscope it looks like bunches of grapes. Then in 1886, Anton J. Rosenbach isolated two *Staphylococcus* strains and one of those strains had gold color colonies (*aureus* in Latin) and due to that fact, it was named *Staphylococcus aureus.* By the 1920s it was discovered that this pathogen has an enzyme capable of clotting plasma, called coagulase, associated with its pathogenicity [49].

When penicillin was introduced for clinical use *S. aureus* was extremely susceptible but, due to its common use in the clinical media, by late 1940s resistant strains started to appear. This led to the development of new therapeutic drugs such as methicillin. By the 1990s high levels of methicillin-resistant *S. aureus* (MRSA) were reported in hospitals (HA-MRSA) as well as emerging cases of community-associated MRSA (CA-MRSA). To treat MRSA, vancomycin is normally used, although it was observed that resistance to this antibiotic was also developed [49]. Nowadays, more than 20 distinct genetic lineages of CA-MRSA are known (reviewed by Watkins *et.al* in 2012) [50]. The USA300 strain is one of the most epidemic strains and it has been reported in more than 50 countries [51,52].

In 2017, World health organization (WHO) did a study of the percentage of invasive isolates of *S. aureus* with resistance to methicillin (MRSA) in Europe (from the available data from 2015-2016) where Romania showed the highest percentage (>50 %), being followed by Portugal, Spain, Italy, Hungary, Greece, Croatia (25 % to <50 %) (WHO 2017).

In Humans, the biggest reservoir of *S. aureus* is the nose, although it is also a common colonizer of the skin, hair, and mucous membranes. Normally these resistant bacteria are not associated with disease. But if the skin barrier is overcome they can cause serious infections that can be either acute or chronic infections, systemic infections or syndromes toxin-mediated [53].

The most common clinic associated infection is from the skin and soft tissue. The infections can be of the epidermis (as impetigo), subcutaneous tissues or of the superficial and deep dermis (e.g. carbuncles). Also, *S. aureus* is capable of wound infections, meningitis, community-acquired and hospital-acquired pneumonia, joint and bone infections [54].

The toxin-mediated syndromes are defined as: menstrual and nonmenstrual staphylococcal; toxic shock syndrome such as food posing are caused by some enterotoxins (reviewed by Bukowski *et. al* in 2010 [55] and by Spaulding *et.al* in 2013 [56]).

1.2.2 Metabolism of *Staphylococcus aureus*

All living organisms need Being a facultative anaerobic bacteria *S. aureus* is capable of performing aerobic and anaerobic respiration [57,58]. Under aerobic conditions the final electron acceptor is oxygen; in anaerobic environments it can perform nitrate respiration or fermentation [58]. This ability of adaptation to distinct growth conditions allows this pathogen to colonize different environments, from the skin to the internal host niches where the availability of free oxygen diminishes [57–59]. During host invasion, *S. aureus* must adapt to the different carbon sources available as well as the oxygen levels present and such fast-metabolic adaptation that this pathogen is capable of is one reason for its higher pathogenicity when compare with other staphylococci [60].

S. aureus uses the glycolytic pathway, the pentose phosphate, and the TCA to perform the catabolism of carbohydrates [57,61]. It is also capable of performing amino acid catabolism, but it appears unable to metabolize fatty acids since it lacks the genes encoding for the enzymes needed for β-oxidation [62,63].

1.2.3 Respiratory chain of *Staphylococcus aureus*

S. aureus is a prominent human pathogen, however its respiratory chain is still poorly understood [57,58]. This pathogen is predicted to have a branched respiratory chain as many other bacteria, having two terminal oxidases to support aerobic respiration [64,65].

Unlike the canonic respiratory chain of mitochondria, the reduction of the oxygen (terminal electron acceptor) is not performed by the cytochrome *c* oxidase but by two terminal menaquinol (MQH_2) oxidases [66,67]: Cytochrome aa_3 oxidase (QoxABCD) which is capable of proton translocation and usually works under aerobic conditions [68,69], and cytochrome *bd* oxidase (CydAB) which is expressed under microaerobic conditions[70] and is not capable of proton-translocation [64,65]. The presence of a third terminal oxidase has also been suggested but no genes encoding for it have been identified (reviewed by Gotz and Mayer in 2013 [71]).

As mentioned before an electron entry point in the respiratory chain is complex I [1,3] however in *S. aureus* no genes encoding for complex I subunits were found in its genome [2].*S. aureus* contains a Type-II NADH:quinone oxidoreductase (NDH-2), which performs the same catalytic function as complex I but is not involved in proton translocation [72–75]. This enzyme is smaller and simpler than complex I and is membrane-associated [72,73].

The capacity of this pathogen to create membrane potential is poorly understood. In 2015 Mayer *et. al* [76] identified a complex composed of three subunits called Membrane potential-generation system (Mps) ABC.

In addition to NDH-2 *S. aureus* has in its genome more genes encoding for quinone reductases such as malate:quinone oxidoreductase (MQO) [77], pyruvate:quinone oxidoreductase (PQO) [78] and succinate:quinone oxidoreductase (SDH) [79]. All these enzymes (MQO, PQO and SDH) catalyse

reactions important either to the TCA and/or respiratory chain. So, it could be said that these enzymes play an important role as a direct link between different metabolic pathways.

A putative respiratory chain of *S. aureus* was hypothesised using the taxonomic profiling from Marreiros *et.al* [1] (Figure 1.2) . Although it is known that a lactate:quinone oxidoreductase [77,80] is present in this organism, it was previously assigned as a malate:quinone oxidoreductase, due to their high amino acid sequence similarity. To simplify the image, monotopic quinone oxidoreductases that were found by the taxonomic profiling are represented in 1.2B. In this profile four different monotopic quinone oxidoreductases were found.

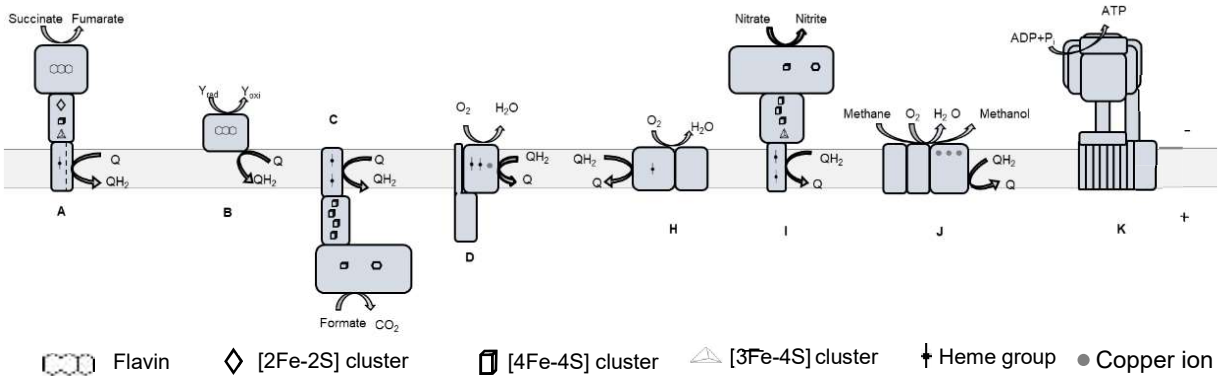

Figure 1.2- ***Staphylococcus aureus* respiratory chain.** Schematic representation of *S. aureus* proteins that are involved in the respiratory chain. Only the monomers are represented in case of homo-oligomers. A- Succinate:Quinone oxidoreductase (SDH); B- Monotopic quinone oxidoreductases (Type 2 NADH:quinone oxidoreductase (NDH-2); Malate:quinone reductase (MQO); dihydroorotate:quinone oxidoreductase (DHODH); Glycerol-3-phosphate:quinone oxidoreductase (G3PDH-GlpD); Pyruvate:quinone oxidoreductase (PQO)); C- Formate:quinone oxidoreductase (Fdn-N); D-Heme-copper oxygen reductases (HCO); H- Cytochrome *bd* oxidase; I- Quinol-nitrate oxidoreductase (NarGHI); J- Particular methane monooxygenase (pMMO), also representing Ammonia monooxygenase; K- F-ATPases Adapted from Marreiros *et.* al [1] for the constructions of this respiratory chain the strain *Staphylococcus aureus* subsp. *aureus* N315 (MRSA/VSSA) was used and only profiles with a score higher than 80 % are represented.

1.2.3.1 Membrane potential generating system (Mps) ABC

As mentioned before, Mayer *et.al* [76] identified one operon containing three genes, *mpsA*, *mpsB* and *mpsC*. The *mpsA* showed sequence homology to *nuoL* sequence from *E. coli*. This *E. coli* protein is believed to be responsible for proton translocation in the membrane arm of complex I [22]. Therefore, the protein encoded by *mpsA* was called NouL-like protein membrane potential generation system (Mps) A. Little is still known about the complex expressed by that operon, but it is suspected that the complex may take a part in conserving energy in *S. aureus*, since the work of Mayer *et.al* [76] demonstrated that

the mutants lacking the three subunits generate lower membrane potential. It was also observed that mutants lacking MpsA or MpsABC had impaired growth [76].

Prior to the work of Mayer *et.al* [76], Marreiros *et.al* [81] identified a gene cluster containing two genes: one encoding for a homologue of NuoL and the other encoding for a periplasmic protein with a domain of unknown function (DUF) called DUF2309. These two proteins identified by Marreiros *et.al* [81] are the MpA and MpsB respectively.

1.2.3.2 Malate:quinone oxidoreductases and Lactate:quinone oxidoreductases

In *S. aureus* two genes encoding two MQOs, *mqoI* and *mqoII* have been reported [77,80].Although the difference between them is not well understood, recent works by Fuller *et.al* [77] showed that the second copy of MQO in the *Staphylococcus aureus* subsp. *aureus* COL (MRSA) (MQOII) is actually a NAD^+-independent lactate dehydrogenase (iLDH), since this enzyme, when purified, had no affinity for malate [80]. Also, it was demonstrated that this enzyme is more important under moderate NO stress, to produce acetate by *L*-lactate oxidation. Formation of acetate yields ATP that is important for amino acid import; MQOI is said to be required for the conversion of malate to oxaloacetate that is a gluconeogenesis precursor [80].

The capability of *S. aureus* to metabolize *L*-lactate by iLDH was known since 1969 [82], this enzyme is responsible for the oxidation *L*-lactate to pyruvate with reduction of quinone. But no gene of iLDH was present in the *S. aureus* genome, since sequence and homology searches using the known iLDH sequence failed to identify a gene encoding an iLDH in this pathogen [77,80].

The MQO and LQO of *S. aureus* are flavin proteins but the exact flavin cofactor (FAD or FMN) has still to be identified [77,80]. In *S. aureus* the MDH enzyme is absent [77] so the oxidation of *L*-malate in this microorganism is only dependent of MQO activity'.

2. Aims

This project aimed to contribute to a better understating of *Staphylococcus aureus*' energetic metabolism by exploring its respiratory enzymes. Three respiratory enzymes were focused in this project: complex MpsAB and two MQOs.

Furthermore, our intended was to understand the biologically function of these enzymes and achieve its purification. In the case of MQOs we expected to further understand their metabolic implication in the bacteria metabolism and for this, cellular studies were performed.

3. Methods

3.1 Expression and purification of MpsAB-6xHisTag

The MpsAB complex is expected to have a molecular mass of 157.88 kDa, with the subunit A (membrane subunit) containing 55.27 kDa and the subunit B (soluble subunit) 102.64 kDa. With the 6xHisTag at subunit B, the overall molecular mass expected for the complex is 158.70 kDa. The molecular mass was calculated using the ExPASsy (Swiss Institute of Bioinformatics, Swiss); the amino acid sequence from USA300_0425 was used to estimate the molecular mass of subunit A, and that from USA300_0426 for subunit B.

3.1.1 Heterologous expression of MpsAB-6xHisTag in *Escherichia coli* strains

With the intent of expressing the complex MpsAB in *E. coli* cells, the gene cluster of interest was cloned in pET21b(+) (Merck) resulting in the addition of a 6xHisTag at the N terminus of subunit B. The construction of this plasmid was done prior my arrival at the laboratory.

In this thesis project a series of expression tests using different *E. coli* strains: C41(DE3) (Lucigen); C43(DE3) (Lucigen) and Lemo21(DE3) (New England Biolabs) were performed. All the *E. coli* strains used are listed in table 3.1.

3.1.2 Preparation and transformation of competent *Escherichia coli* strains

Chemically competent *E. coli* cells C41(DE3), C43(DE3) and Lemo21(DE3) were prepared from 20 mL of an overnight culture growth in Luria Bertani Broth (LB) (Table S1) at 37 °C, 150 rpm. From this overnight culture, 500 µL were inoculated in 50 mL of Super Optimal Broth (SOB) medium (Table S1) supplemented with 500 µL of the magnesium solution (200 g/L calcium chloride, 250 g/L magnesium sulphate) and incubated at 37° C, 150 rpm. The culture growth was stopped by incubating it in ice for 10 minutes, when the optical density at 600 nm (OD_{600nm}) (measured with an Amersham Biosciences Ultra Spec 10 Cell Density Meter) reached 0.6. Then, the culture was centrifuged at 2100 x g, 4 °C for 10 minutes. The obtained pellet was resuspended in 16 mL of sterile and cooled Tris-Borate (TB) buffer (10mM 4-(2-hydroxyethyl)-1-piperazineethanesulfonic acid (Hepes), 15 mM calcium chloride, 250 mM potassium chloride, 55 mM magnesium chloride). The resuspended pellet was kept in ice for 10 minutes, followed by a centrifugation at 2 100 x g, 4 °C for 10 minutes. The new obtained pellet was resuspended in 4 mL of sterile and cooled TB buffer. Dimethyl sulfoxide (DMSO) was added to a final concentration of 7 % (v/v) and the mixture was further incubated on ice for 10 minutes. The cells were aliquoted, frozen in liquid nitrogen and stored at -80 °C [83].

For the three strains tested, cells were transformed with the vector containing the gene cluster of *mpsAB* or with the empty vector as control.

To transform chemically competent *E. coli* strains, 1 µL of the construct was added to 50 µL of thawed competent cells and kept on ice for 30 minutes. Then cells were heat-shocked at 42 °C for 45 seconds and incubated on ice for 2 minutes followed by addition of 950 µL SOC medium (SOB supplemented with 20.6 µM glucose and 20.6 µM magnesium chloride). The cell suspension was incubated at 37°C for 1 hour and 30 minutes followed by a centrifugation for 5 minutes at 2 400 x g from which 900 µL of the supernatant were discarded and the remaining supernatant was used to suspend the pellet and plated on LB agar supplemented with 100 µg/mL ampicillin. In the case of LEMO21(DE3) cells the plates were also supplemented with 30 µg/mL chloramphenicol. The plates were incubated at 37 °C overnight [83].

Table 3.1- ***E. coli*** **strains used in this study with their respective characteristics.**

Bacterial strain	**Relevant Characteristics**	**Source/Reference**
E. coli		
OverExpressC43 (DE3)	Derived from BL21 (DE3). F^- ompT gal dcm $hsdS_B(r_B^- m_B^-)$(DE3)	Lucigen
OverExpressC41(DE3)	Derived from C41 (DE3) F^- ompT gal dcm $hsdS_B(r_B^- m_B^-)$(DE3)pLysS (Cm^r) *fhuA2 [lon] ompT gal (λ DE3) [dcm] ΔhsdS/ pLemo*(Cam^R)	Lucigen
LEMO21 (DE3)	*λ DE3 = λ sBamHIo ΔEcoRI-B int::(lacI::PlacUV5::T7 gene1) i21 Δnin5* pLemo = pACYC184-*PrhaBAD-lysY*	New England Biolabs
DC10B [a]	Δ*dcm* in the DH10B background; Dam methylation only	New England Biolabs

Note: [a] Cells used in sector 3.2.2

3.1.3 Expression tests

In the case of C41(DE3) and C43(DE3) expression tests were made from an overnight culture grown at 37 °C, 150 rpm in Yeast extract and Tryptone (2YT) medium (Table S1) supplemented with 100 µg/mL ampicillin. In the next day, 2% of the overnight culture was inoculated in 20 mL of 2YT supplemented with 100 µg/mL ampicillin at 37 °C, 150 rpm and grown until an OD_{600nm} of to 0.4, followed the addition of 200 µM of Isopropyl β-D-1-thiogalactopyranoside (IPTG) and the growth continued for 24 more hours.

To see how the growth temperature could influence the protein expression, the same condition was tested but when the cells reached an OD_{600nm} of 0.4 the growth was cooled to 20 °C [84] followed by addition of the same IPTG concentration. The growth continued for 24 more hours.

For all the expression tests performed a 1 mL aliquot were taken before induction and every two hours after the addition of IPTG till six hours growth after induction and then after 24 hours and stored at – 20 °C.

The LEMO21(DE3) strain contains the pLEMO plasmid which encodes for the natural inhibitor of T7 RNA polymerase (RNAP), T7 lysozyme (lys) which is controlled by the well-titratable *L*-rhamnose promoter and also encodes the chloramphenicol resistance marker [85]. So, in this strain, the optimal *L*-rhamnose concentration for the protein expression has also to be determined. Expression tests with different *L*-rhamnose concentrations 0 µM; 50 µM; 500 µM and 2000 µM were tested. The growths were made at 37 °C, 150 rpm in LB until an OD_{600nm} of 0.4, then 400 µM IPTG were added and the growth proceeded at 22.5 °C,185 rpm for 24 hours.

The subsequent expression tests were done without *L*-rhamnose. To optimize the expression of the protein complex the IPTG concentration, the medium and stirring speed were evaluated. A summary of the conditions tested are listed in table 3.2

Table 3.2 -**Summary of the screening tests made after having chosen the concentration of *L*- rhamnose.**

Medium	***LB***	***LB***	***LB***	***LB***	***2YT***	***2YT***
T till OD_{600nm} 0.4 (°C)	37	22.5	30	30	37	37
T Induction (°C)	22.5	22.5	30	30	22.5	22.5
IPTG (µM)	200	400	400	400	400	200
stirring speed (rpm)	185	185	150	180	185	185

The expression of the mpsAB-6xHisTag complex was analyzed by 12 % acrylamide sodium dodecyl sulfate-polyacrylamide gel electrophoresis (SDS-PAGE).

The aliquots taken during each growth of the different screening tests were normalized to an OD_{600nm} of 0.4 before loading in the SDS-PAGE. This normalization allows the comparison of the expression in each condition. The samples were then centrifuged at 2 400 x g for 5 minutes at room temperature, the obtained pellet was resuspended in 25 µL loading buffer (4 mL 500 mM tris hydrochloride pH 8.00; 0.8 g SDS; 0.04 g bromophenol blue; 4.6 mL glycerol; 400 µL β-mercaptoethanol; 8M urea) followed by an incubation at 46 °C for 30 minutes [84]. Then, 12 µL of each sample were loaded in the acrylamide gel.

3.1.5 Scale-up growth of the selected expression condition

A scale-up growth was performed using the LEMO(DE3) strains grown in 2YT medium supplemented with 100 µg/mL ampicillin at 37 °C, 185 rpms. The expression of the complex was induced with 400 µM IPTG when the OD_{600nm} reached 0.4 and then cells were cooled to 22.5 °C. The growth continued for six hours after induction.

3.1.6 Purification of MpsAB-6xHisTag

Thawed cells of the scale-up growth were resuspended in 50 mM sodium phosphate dibasic/sodium phosphate monobasic buffer -phosphate buffer (KPi)- pH 7.50, 150 mM NaCl, 1 mM EDTA and 100 mM phenylmethanesulfonyl fluoride (PMSF). The French press was used to disrupt the cells (41.4 MPa) and cellular debris and undisrupted cells were separated by a centrifugation at 22 100 x g for 15 minutes. To separate the membrane fraction from the soluble fraction an ultra-centrifugation at 219 333 x g for 2 hours was made. The pellet corresponding to the membrane fraction was resuspended in the same buffer. The proteins in the membrane fraction were then solubilized with n-Dodecyl-β-D-Maltoside (DDM) detergent in a final concentration of 1 % (w/w) [86]. After an overnight incubation with DDM at 4 °C with gentle shaking the separation of the solubilized fraction from the non-solubilized fraction was achieved with an ultra-centrifugation at 219 333 x g for 2 hours.

The membrane solubilized fraction was injected into a Hi-Trap IMAC HP 5mL (GE Healthcare) charged with 0.15 M nickel sulfate. The elution was done using a *L*-histidine gradient (0 to 250 mM) in 50 mM KPi pH 7.50, 500 mM NaCl, 0.05 % DDM.

All the columns used in this study were operated by an AKTA Prime PLUS system (GE Healthcare) and the elution of protein was monitored by the change in absorbance at 280 nm.

UV-visible absorption spectroscopy was used to evaluate the different protein fractions resulting from the purification steps. All the UV-visible spectra were acquired on a Shimadzu UV-1800 spectrophotometer, at room temperature, using a wavelength range from 250 to 750 nm.

The purity of the different samples was analyzed in a 12 % acrylamide SDS-PAGE according to standard procedures [84].

Protein quantification was performed using the Biuret Protein Assay following the standard protocol [87].

The identification of proteins by Mass Spectrometry (MS) was performed at the Mass Spec Facility UniMS, ITQB-NOVA, Oeiras, Portugal.

3.2 Purification of MQO I and MQO II of *Staphylococcus aureus*

For the study of MQOI and MQOII, the encoding genes were previously cloned in pET28a(+) (Genscrip). The vector was then transformed in Rosetta (DE3) cells. The expression of these proteins was previously done in laboratory and cells were kept at -20 °C.

3.2.1 Purification procedure

To performed the purification of MQOI and MQOII, 53 g and 82 g of Rosseta (DE3) cells respectivelly, were thawed and resuspended in 50 mM KPi buffer pH 7.00, 10 % glycerol, 300 mM sodium chloride, 1 mM EDTA, 100 µM PMSF were disrupted using a French Press at 41.1 MPa. Separation of disrupted cells from non-disrupted was achieved by centrifugation at 22 100 x g for 10 minutes.

The supernatant was collected and an ultracentrifugation at 219 333 x g for 2 hours was performed to separate the membranes from the soluble fraction. The soluble fraction was collected and stored at 4 °C and the membrane pellet was resuspended in 50mM KPi buffer pH 7.00, 10 % glycerol, 2 M NaCl, 100 µM PMSF with a Potter homogenizer.

The resuspended membrane fraction was kept in the same buffer overnight at 4 °C with gentle stirring. Since MQO's are believed to be monotopic proteins, their release from the membrane could be achieved using high ionic strength. The high ionic strength would disturb the electrostatic forces that keep the protein in the membrane. The fraction that corresponds to the proteins whose electrostatic forces were disrupted will be denominated washed membrane fraction.

To separate the membrane fraction from the washed membrane fraction an ultracentrifugation at 219 333 x g for 2 hours was made. The ionic strength of the last fraction was decreased to 300 mM by adding 50 mM KPi buffer pH 7.00,10 % glycerol and 100 µM PMSF. To concentrate the sample an ultrafiltration device with a 30 kDa membrane (Millipore) was used. All of this process was done at 4 °C.

The soluble and the washed membrane fractions were, separately, injected into a 5mL HiTRAP IMAC (GE Healthcare) and the elution was performed using an *L*-Histidine gradient (0 mM to 250mM) in 50 mM KPi buffer pH 7.00, 10 % glycerol, 300 mM NaCl.

In the case of MQOII, a different approach was also tried. The methods for the disruption the cells and separation of the soluble fraction and membranes were as described above. But instead of 2 M sodium chloride for the disturbing of the electrostatic forces of the monotopic proteins only 1 M was used. After having the membrane pellet it was resuspended using a Potter homogenizer in 50 mM KPi buffer pH 7.00, 10 % glycerol,100 µM PMSF and 1 M NaCl, and was kept at 4 °C with gentle stirring overnight. The ionic strength of the membrane fraction was reduced to 500 mM with successive ultracentrifugations at 219 333 x g for 2 hours. The obtained membrane pellet was resuspended in 50 mM KPi buffer pH 7.00, 10 % glycerol, 100 µM PMSF. When the membrane fraction had the desired

ionic strength the membrane pellet was solubilized in 1 % (w/w) DDM [84] at 4 °C with gentle shaking. To separate the solubilized protein from the non-solubilized protein an ultracentrifugation at 219 333 x g for 2 hours was performed, and the obtained membrane pellet was resuspended in 50 mM KPi buffer pH 7.00,10 % glycerol, 100 µM PMSF, 500 mM NaCl and 0.05 % DDM.

The solubilized membrane fraction was then injected in a 5mL HiTRAP IMAC (GE Healthcare) charged with zinc instead of nickel, and the elution was made as described above.

The purity of the different samples was analyzed in a 12 % acrylamide SDS-PAGE according to the protocol standard protocol[88], for solubilizing proteins the same protocol as described above was used [84].

The protein quantification was done by the biuret assay [87].

3.2.2 Functional Characterization

3.2.2.1 Lactate:2,6-Dichlorophenolindophenol (DCPIP) oxidoreductase activity of MQOII

Steady-state enzymatic assays were performed under aerobic conditions. Each condition was performed in triplicate at 25 °C and with continuous stirring. The reduction of the electron acceptor DCPIP (Sigma Aldrich) was measured spectroscopically in a Shimadzu UV-18000 by following the decrease of the absorbance at 600 nm (ε_{600nm} =20.7 mM^{-1} cm^{-1} [89]) . In each assay 50 mM DCPIP in 50 mM KPi pH 7.00 and 500 mM sodium chloride, were mixed with 50 nM of protein, and the assay started with the addition of potassium lactate.

Enzymatic activity was also measured in the presence of 2-n-Heptyl-4-hydroxyquinoline-N-oxide (HQNO) a quinone analog that acts as an inhibitor to quinone reductases.

The concentration of protein was determined by the absorbance at 450 nm of the FAD cofactor (ε_{450nm}= 11 300 M^{-1} cm^{-1} [90]).

3.3 Cellular studies of MQOI and MQOII in Energetic metabolism of *Staphylococcus aureus*

To understand the impact of MQOI and MQOII in the energetic metabolism of *S. aureus*, bacterial growths of a wild-type strain and of a mutant with a transposon in the gene coding for *mqoI* or for the *mqo*II, respectively, were performed.

The *S. aureus* strains used in this study are listed in table 3.3

Table 3.3- ***S. aureus*** **strains used in this study with their respective characteristics.**

Bacterial strain	Relevant Characteristics	Source/Reference
S.aureus		
SAUSA300 JE2	Homogeneous HA-MRSA strain	University of Nebraska Medical Center
SAUSA300_2541 MQOI::*Tn*	Homogeneous HA-MRSA strain transposon mutant. It is the product of an insertion, resulting in a erythromycin-resistant strain of JE2, that causes the disruption of SAUSA300_2541, which encodes for the MQOI protein	University of Nebraska Medical Center
SAUSA300_2312 MQOII::*Tn*	Homogeneous HA-MRSA strain transposon mutant. It is the product of an insertion, resulting in a erythromycin-resistant strain of JE2, that cause the disruption of SAUSA300_2312, which encodes for the MQOII protein	University of Nebraska Medical Center

3.3.1 Cell Growth

S. aureus strains obtained from the Nebraska Transposon Mutant Library were grown in Tryptic Soy Agar (TSA) (Table S2). The strains with a transposon were selected with 25 µg/mL of erythromycin (Roth).

The growths were made in a chemical define media (CDM), composition (Table S3) and preparation in Supporting Information [91–93].

For the overnight culture from CDM growth, a single colony from the TSA plate was inoculated. The growth was then inoculated to have an initial $OD_{600nm\ of}$ 0.05 and was grown for 8 hours at 37° C, 200 rpm.

For all the cellular growths, the OD_{600nm} was measured using a cell density meter (Amersham Biosciences) and the pH (pH meter GLP 22; Crison Instruments, SA). Measurements were done at 1 - hour intervals and biological triplicates of each strain were made.

In the CDM three carbon sources were tested; 5mM *D*-glucose (extra pure, Scharlau), CDMG; 5 mM sodium acetate (Panreac), CDMA; and 5 mM potassium *L*-lactate (FLUKA), CDML. The growth conditions were done in a 1:10 liquid-to-air ratio.

For metabolite nuclear magnetic resonance analyses, *S. aureus* growth in CDMG was used. This growth was done in a 1:5 liquid-to-air ratio for 8 hours at 37 °C, 200 rpm and a sample of 1.5 mL was taken every 1 hour, centrifuged (16 200 x g, 5 minutes at 4 °C) and the supernatant, as well as the cells pellets, were stored at -20 °C.

The handling of *S. aureus* was always performed in a laminar flow chamber (Class II Type A/B3 Laminutesar Flow biological safety cabinet, Nuaire).

3.3.2 NMR-Based Metabolomics

3.3.2.1 Sample preparation

For the extracellular metabolome ^{1}H-NMR analysis 5 mm glass tubes (NORELL 508-UP) were used. For the preparation of the sample, to 400 µL of each collect supernatant 66 mM di-sodium hydrogen phosphate/potassium dihydrogen phosphate buffer pH 7.00 prepared with 100 % deuterium oxide (D_2O; CortecNET) were added in order to achieve the NMR-lock signal . Also, 1 mM 3-trimethylsilyl-[2,2,3,3-D4]-1-propionic acid (TSP, UvasolV®) was used as the internal standard for chemical shift referencing, quantification and normalization of NMR peak intensities.

3.3.2.2 NMR data collection

All the NMR data was acquired at the CERMAX, ITQB-NOVA, Oeiras, Portugal

All the ^{1}H-NMR spectra acquisition were made at 25 °C using a Bruker AVANCE III 500 NMR spectrometer, with a central frequency of 500.13 MHz (Bruker Biospin). This spectrometer is equipped with a 5 mm TCI C/N Prodigy Cryoprobe (Bruker).

Topspin version 3.2 software (Bruker Biospin) was used to control the equipment. The spectra were obtained with water presaturation during a delay of 2 s and a using a total recycling time of 35 s to achieve a total relaxation of the signals. In total eigthy-seven spectra were collected. All spectra were collected into 64 K data points using a spectral width of 16 ppm. No exponential multiplication was performed when doing the Fourier transform.

3.3.2.3 NMR data analyses and quantification

The analysis of the ^{1}H-NMR spectra was performed using *Topspin version 3.2 software* (Bruker Biospin) with phase and the baseline correction and the signal of TSP was set to have a chemical shift of δ=0.00 pm.

Compound identification was performed using *Chenomx NMR Suite version 8.11 software* (Chenomx Inc.). The identification was performed by matching the spectra of standard compounds in the program database with the ^{1}H-NMR spectra acquired. This program was also used to do the quantification of the compounds. For each spectrum acquired the chemical shape indicator was set to 1 mM of TSP and the peak center, height and width were defined.

3.3.3 Promoter fusion molecular cloning

3.3.2.1 Sample preparation

The primers used in this study to construct the GFP promoter fusion are listed in Table 3.4 The restriction sites are underlined and in bolted.

Table 3.4- **Primers used in this study. The restriction sites are underlined and in bolted.**

Primer name	Sequence (5'-3')	Restriction Enzyme
P1-UpMqo2312-EcoRI	ATA**GAATTC**TCACAACTTATGGTGGTTTAAGTG	EcoRI
P2-UpMqo2312-sGFP	TCCTTTACTCATATTAATACCACTTTAAATCAATAAG	
P3-UpMqo2312-sGFP	AGTGGTATTAATATGAGTAAAGGAGAAGAACTTTTC	
P4-sGFP bward XmaI	CGCG**CCCGGG**TTAATGGTGATGATGGTGATGG	XmaI
P1-UpMqo2541-EcoRI	AAT**GAATTC**ATAGCAATCAATAAACATAGCAAAG	EcoRI
P2-UpMqo2541-sGFP	TCCTTTACTCATTGGTTTCACCTCTCCAAAAATTG	
P3-UpMqo2541-sGFP	AGAGGTGAAACCAATGAGTAAAGGAGAAGAACTTTTC	

The plasmids used in this study are listed below with their relevant characteristics, Table 3.5.

Table 3.5- **Plasmids used in this study with their relevant characteristics.**

Plasmid	Relevant Characteristics	Source/Reference
pFAST3	Plasmid encoding fast-folding *GFP*(P7), a derivative of pSG5082; Amp^r, Ery^r	Nair *et. al* [94]
pSP64E	*E.coli* plasmid; Amp^r	Promega
pSP64E+mqoII_GFP	Psp64E derivative encoding the *mqoII* promoter fused with GFP	This study
pSP64E+mqoI_GFP	Psp64E derivative encoding *mqoI* promoter fused with GFP	This study

3.3.2.2 Extraction of genomic DNA from *S. aureus* JE2

Genomic DNA from *S. aureus* was purified from cells grown overnight on TSA, at 37 °C. Cells were resuspended in 50 mM EDTA and incubated at 37° C for 30 minutes in the presence of Lysostaphin (Sigma, 10 µg/mL) and RNase (Sigma, 20 µg/mL). Cells were then incubated at 80 °C for 5 minutes with EDTA 50 mM and Nuclei Lysis solution (Promega). Cells were cooled to room temperature and Protein Precipitation solution (Promega) was added and incubated for 10 minutes. Samples were then centrifuged at 16 200 xg for 20 minutes at room temperature and the supernatant was transferred to a microcentrifuge tube containing isopropanol (Sigma) at room temperature. After a gentle mix by inversion the samples were centrifuged at 16 200 xg for 10 minutes. The supernatant was discarded and ethanol (Sigma) 70 % was added followed by a centrifugation at 16 200 xg for 3 minutes. After discarding, the supernatant, the pellet was air-dried for 5 minutes and was resuspended in water. The gDNA was then quantified and stored at – 20 °C.

All DNA quantification was performed using a NanoDrop Spectrophotometer (ThermoFisher).

3.3.2.3 Overlapping Polymerase chain reaction (PCR) to obtain the insert promoter with GFP

The primers used in this study were ordered from Metabion Internation AG and are listed in table 3.4. All the PCR reactions were performed in the MJ Mini™ Thermo Cycler (Bio-Rad).

To obtain the promoter fused to GFP at the 5' end an overlapping PCR was created. First, each promoter region of *mqoI* and *mqoII* were amplified from gDNA of *S. aureus* and the GFP was amplified from the pFAST3 plasmid.

Four reaction mixtures were prepared for a total volume of 50 µL with 0.2 µM dNTPs (Sigma), 0.5 µM of each primer (for the amplification of each promoter its respective P1 and P2 were used, and for sGFP P3 and P4) , 250 ng of template DNA (gDNA for the promoter and pFAST3 for sGFP), 1x Phusion Phusion High-fidelity DNA polymerase Buffer (Finnzymes,ThermoFisher) and 0.02 U Phusion High-fidelity DNA polymerase (Finnzymes,ThermoFisher).

The PCR program used had an initial denaturation step at 98 °C for 1 minute, followed by 20 cycles of denaturation at 98 °C for 10 seconds, annealing at 56 °C for 30 seconds, extension at 72 °C for 30 seconds, and a final extension at 72 °C for 7 minutes. The PCR products were purified using the Wizard® SV Gel and PCR Clean-Up System (Promega) according to the manufacturer's instructions, and the elution of the PCR product was made using ddH_2O. The purified PCR product was quantified and stored at -20 °C.

Next, each amplified promoter of *mqo2312* and *mqo2541* was fused with the amplified sGFP by PCR obtaining the desired insert to ligate the pSP64E plasmid.

Separate reactions were made in a total volume of 50 µL, by adding 0.2 µM dNTPs (Sigma), 0.5 µM of each primer (P1 and P4), 100 ng of each amplified product (desired promoter and sGFP), 1X Phusion High-fidelity DNA polymerase Buffer (Finnzymes,ThermoFisher) and 0.02 U of Phusion High-fidelity DNA polymerase (Finnzymes,ThermoFisher)

The PCR program used was similar to that described above, with the exception that instead of 20 cycles 25 cycles were performed.

3.3.3.4 Restriction digests of plasmid and PCR fragments

Plasmidic DNA and inserts were digested with restriction enzymes from New England Biolabs for cloning. After cloning, restriction analyses of the obtained clones were performed with the same enzymes. For cloning and restriction analyses, reactions were prepared using 100 ng of DNA, 0.4 µM of each restriction enzyme EcoRI-HF® and XmaI, 1X CutSmart® Buffer, and ddH_2O to a final volume of 50 µL. Reactions were incubated at 37 °C overnight and heat-inactivated for 20 minutes at 65 °C in a dry block thermostat (Grant). The digested products using in cloning procedures were purified using the Wizard® SV Gel and PCR Clean-Up System (Promega) according to manufacturer instructions. The digested products were quantified using a NanoDrop Spectrophotometer (ThermoFisher) and stored at -20 °C.

3.3.3.5 Ligation of digested plasmid and promoter insert

Ligation of the pSP64E with the desired *mqo2312_GFP* or *mqo2541_GFP* was performed in a final volume of 20 µL using a 20-fold-excess of insert, 0.02 U T4 DNA ligase (New England Biolabs), 1X T4 DNA ligase buffer and ddH_2O to achieve the final volume. The reaction was incubated at 16 °C

overnight in a thermomixer (Eppendorf) and heat-inactivated for 10 minutes at 65 °C in a dry block thermostat (Grant).

3.3.3.6 DNA and PCR products purity evaluation

1 % agarose gel was used to assess the genomic DNA and PCR products quality and purity as the digested products quality.

The sample (50 ng) was resuspended in 1X gel loading buffer, purple (New England Biolabs) and loaded in the agarose gel. The agarose gel was pre-stained with 0.5 X SYBR® Safe DNA gel stain (Invitrogen). The sample ran for 45 minutes in 1X TAE pH 8.50 (242 g/L TRIS, 5.71 % (v/v) glacial acetic acid, 0.05 M EDTA pH 8.00). The gel was revealed using the Gel Doc™ Imaging system (Bio-Rad) and its image acquisition was done using the Bio-Rad Laboratories Image Lab software (Bio-Rad).

3.3.3.7 Preparation and transformation of competent *E. coli* DC10B cells

Chemically competent *E. coli* DC10B (New England Labs) cells were prepared from 20 mL of an overnight culture growth in LB at 37 °C 150 rpm. From this overnight culture, 1 % was inoculated in 70 mL of LB and was incubated at 37 °C, 150 rpm until an OD_{600nm} of 0.6. Then the culture was centrifuged at 2 400 xg for 5 minutes at room temperature. The obtained pellet was resuspended in 750 µL of cooled sterile 100 mM Calcium chloride followed by 1-hour incubation on ice. A new centrifugation at 2 400 xg for 5 minutes at room temperature was made and the obtained pellet was resuspended in 100 µL of sterile and cooled 100 mM Calcium chloride followed by 1-hour incubation on ice. The cells were used immediately [88].

To transform chemically competent *E. coli* DC10B cells the standard transformation protocol was used [83], and the cells were plated on LB agar plates supplemented with 100 µg/mL ampicillin.

3.3.3.8 Colonies screening for positives constructs

Single colonies were picked and suspended in 50 µL of sterile ddH_2O, 25 µL were heated for 5 minutes at 100 °C ;1 µL was used in the colony PCR. The other 25 µL were kept on ice and if positive for the presence of the construct, were inoculated in LB media supplemented with 100 µg/mL ampicillin and incubated overnight at 37 °C, 150 rpm

To confirm the presence of the desired construct (pSP64E+mqo2312_GFP or pSP64E+mqo2541_GFP) in the colonies, PCR were made using P1 and P4. The PCRs were made to a final volume of 25 µL, adding 1x Master Mix (VWR), 0.2 µM of each primer, 1 µL of heat colony and ddH_2O to complete the volume.

The PCR program used had an initial denaturation step at 95 °C for 2 minutes, followed by 30 cycles of denaturation at 95 °C for 30 seconds, annealing at 56 °C for 40 seconds and extension at 72 °C for 1 minute and 28 seconds, and a final extension at 72 °C for 5 minutes. Then, 5 µL of PCR products were

loaded directly on an 1 % agarose gel and ran for 45 minutes in 1X TAE. The gel was revealed as described above.

3.3.3.9 Purification of plasmid DNA from *E. coli* DC10B

Plasmidic DNA (pSP64E+mqo2312_GFP or pSP64E+mqo2541_GFP) was purified from an overnight culture grown on LB media supplemented 100 µg/mL ampicillin at 37 °C,150 rpm. The extraction was done using the NZYminiprep Kit (NZYTech) following manufacturer's instructions. The plasmidic DNA was eluted with ddH_2O. The purified plasmid was quantified and stored as described above.

4.Results and Discussion

4.1 The MpsABC complex

Subunit A of the MpsAB complex was shown to have sequence homology to the NuoL [76] subunit of complex I from *E.coli*, a membrane subunit proposed to be able of ion translocation. Due to this homology it was hypothesized that MpsA could also translocate ions, but the function of the other subunit of the complex is not understood. As mentioned before, the mutants lacking MpsA or the whole complex have impaired growth, a characteristic associated with Small variant (-like) strain of *S. aureus*.

4.1.1 Heterologous expression of MpsAB-6xHisTag

The overexpression of a membrane protein normally involves its accumulation in the cytoplasmic membrane, which can be toxic for the cells. Another way of expressing membrane proteins is in inclusion bodies although a non-functional protein is often obtained and refolding to a functional one may not be successful [95,96].

The first *E. coli* strains used to perform the expression of the MpsAB-6xHisTag were the Walker strains C41(DE3) and C43(DE3) that are derivatives of the strain BL21. This option took into account the fact that these strains are described to be most suitable for membrane protein expression [84]. As mentioned before an empty vector was also transformed to be the expression control.

Either in C43(DE3) or C41(DE3), the expression of the membrane complex was not detected since in the SDS-PAGE the lanes corresponding to its expression were similar to the controls. (Figure S1)

E. coli LEMO21(DE3) is also a derivative strain of BL21(DE3) [95]. This strain contains the pLEMO plasmid which encodes the natural inhibitor of the T7 RNAP, T7 lys which is regulated by the well-titratable *L*-rhamnose promoter; this plasmid also contains the chloramphenicol resistance marker [85].

In the first expression trial using the LEMO21(DE3) cells, different *L*-rhamnose concentrations were tested: 0μM; 50 μM; 500 μM and 2000 μM. These tests were made in LB media and the expression was induced with 400 μM IPTG when OD_{600nm} reached to 0.4 (Figure S2).

When no *L*-rhamnose was added to the medium (Figure 4.1/ Figure S2) a band with higher intensity above the band of 97.4 kDa of the marker was observable and was assumed to be subunit B, which expected molecular mass is 102.64 kDa. More expression conditions were tested having no *L*-rhamnose in the medium to check if expression could improve. On these new conditions different IPTG concentrations, growth temperature and stirring speed were tested (Table 4.1).

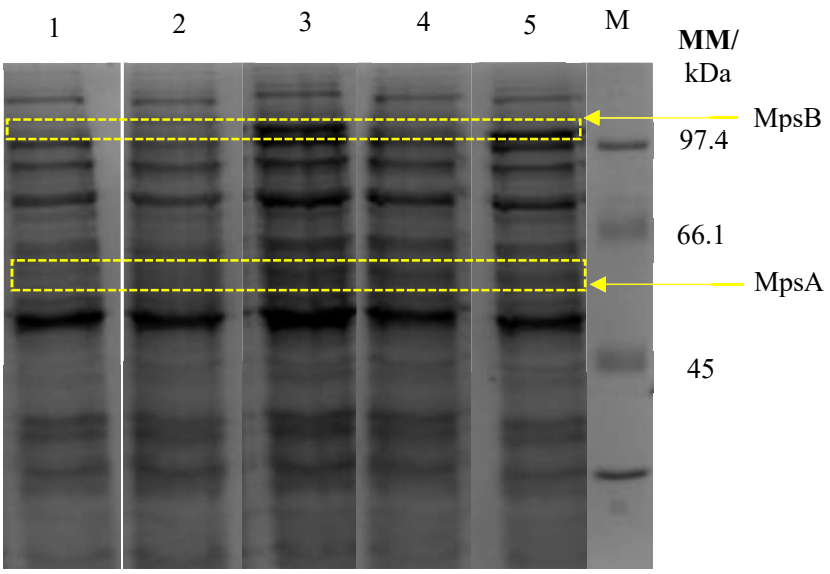

Figure 4.1- **Expression test with no *L*-rhamnose in the medium**. Acrylamide 12 % SDS-PAGE, all the samples loaded in the gel were normalized to an OD_{600nm} of 0. 4. Lane 1: Lemo21(DE3) before ITPG adition; Lanes 2 and 3: Lemo21 after 3 hours of protein induction with pET 21(+)b and pET 21(b)+mpsAB-6xHisTag respectively; Lane 4 and 5 : Lemo21 after 6 hours of protein induction with pET 21(+)b and pET 21(b)+mpsAB-6xHisTag respectively; M: Protein Marker low-range (BioRad).

For all tested conditions the OD_{600nm} was monitored after induction (Figure S3). To understand differences in protein expression an SDS-PAGE was performed (Figure 4.2) with all samples normalized to the same OD_{600nm} (0.4). Expression of subunit B seems to be more evident in the gel than subunit A.

Observation of both the expression results on SDS-PAGE and OD_{600nm} demonstrated higher complex expression in condition C (see table 4.1). In this condition LEMO21(DE3) cells are grown in 2YT medium at 37 °C until OD_{600nm} reaches 0.4, afterwards 400 µM IPTG are added and the growth continued for more six hours. Therefore, it was chosen to perform the scale-up growth with the intent to purify the complex.

Table 4.1-**Summary of the screening tests that appeared to have complex expression.**

Condition	A	B	C	D	E	F
Medium	**LB**	**LB**	**2YT**	**2YT**	**LB**	**LB**
T till OD_{600nm} 0.4 (°C)	22.5	22.5	37	37	30	30
T. Induction (°C)	22.5	22.5	22.5	22.5	30	30
IPTG (µM)	200	400	400	200	400	400
Stirring Speed (rpm)	185	185	185	185	150	180

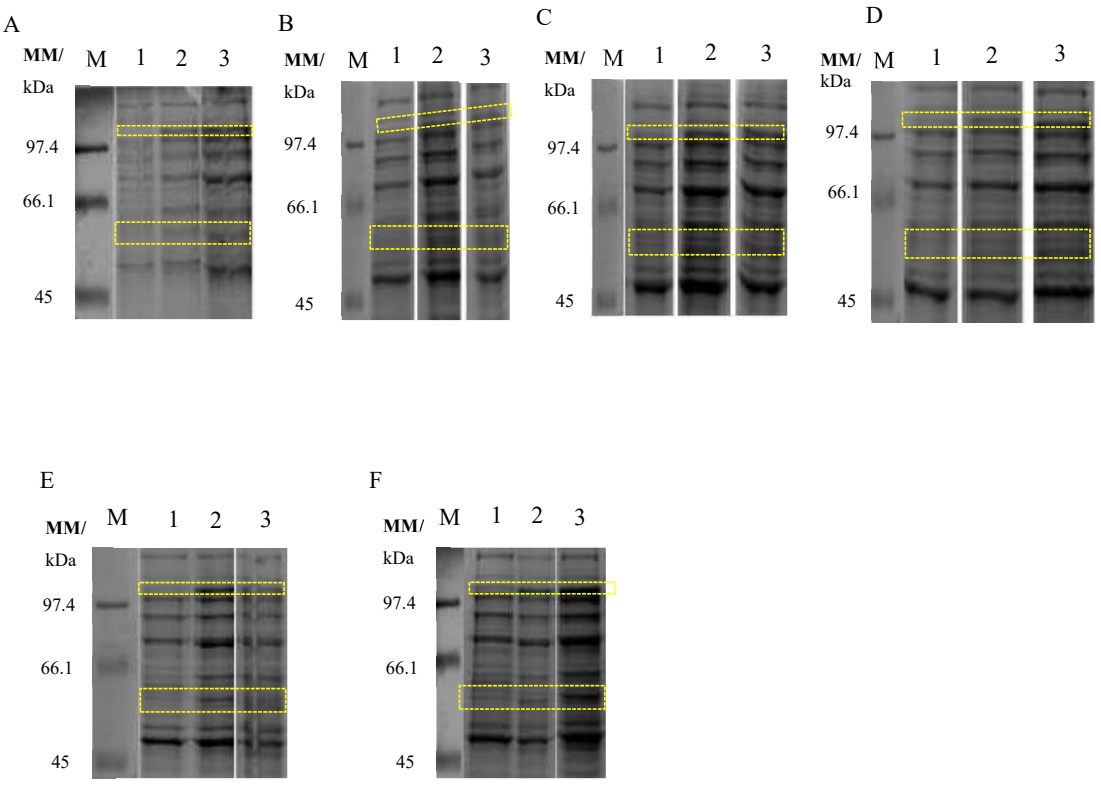

Figure 4.2- **Expression tests comparison.** 12.5 % Acrylamide SDS-PAGE. Each image from A to F represents the expression conditions labelled with the same letter (Table 4.1). For all the SDS-PAGE lane 1, before induction of protein expression; Lane 2, four hours after induction of protein expression; lane 3, six hours after induction of protein expression and M, Protein Marker low-range (BioRad). Yellow dashed boxs marks the expected position of MpsB (102.64 kDa) and MpsA (55.27 kDa)

4.1.2 Purification of MpsAB complex

Membrane proteins are hydrophobic proteins and to keep them in a water-soluble state to perform their purification detergents have be added. Detergents have an amphipathic structure, meaning that they have a hydrophobic and a hydrophilic part. This makes them capable of interacting with the membrane proteins forming a protein/detergent complex in the solubilization process [84]. The detergent chosen to solubilize the MpsAB complex was n-Dodecyl-β-D-Maltoside (DDM).

The subunit B of the complex has a 6xHisTag at the N-terminal. An immobilized metal ion affinity chromatography (IMAC) was used to take advantage of the histidine affinity to the metal. In this case, a HiTRAP charged with nickel was used.

In the chromatogram (Figure 4.3a) the formation of an intense peak at 22 mM histidine (9 % B) is observed. To verify the protein purity of the different fractions collected during the purification an SDS-PAGE was performed. As seen in Figure 4.3b the protein eluted with 22 mM histidine has a band above the 97.4 kDa marker possibly corresponding to subunit B; and another between the 66.2 kDa and 45 kDa markers, which may be subunit A.

This fraction was then concentrated using an Amicon 100 kDa and the UV-Visible spectrum was traced (Figure 4.3C) - a peak was observed at 410 nm which could indicate a contamination of the sample with cytochrome from *E.coli* [97].

To improve the purity of the fraction of interest, it was re-injected in a HiTRAP column in the same conditions; in the following SDS-PAGE gel (Figure 4.4) no band with higher molecular mass than the 97 kDa marker was observed but instead a band with the same molecular mass as the marker was present; mass spectrometry (MS) analyses were made. A negative response was obtained (Figure S4), indicating that the protein was probably lost in the flowthrough.

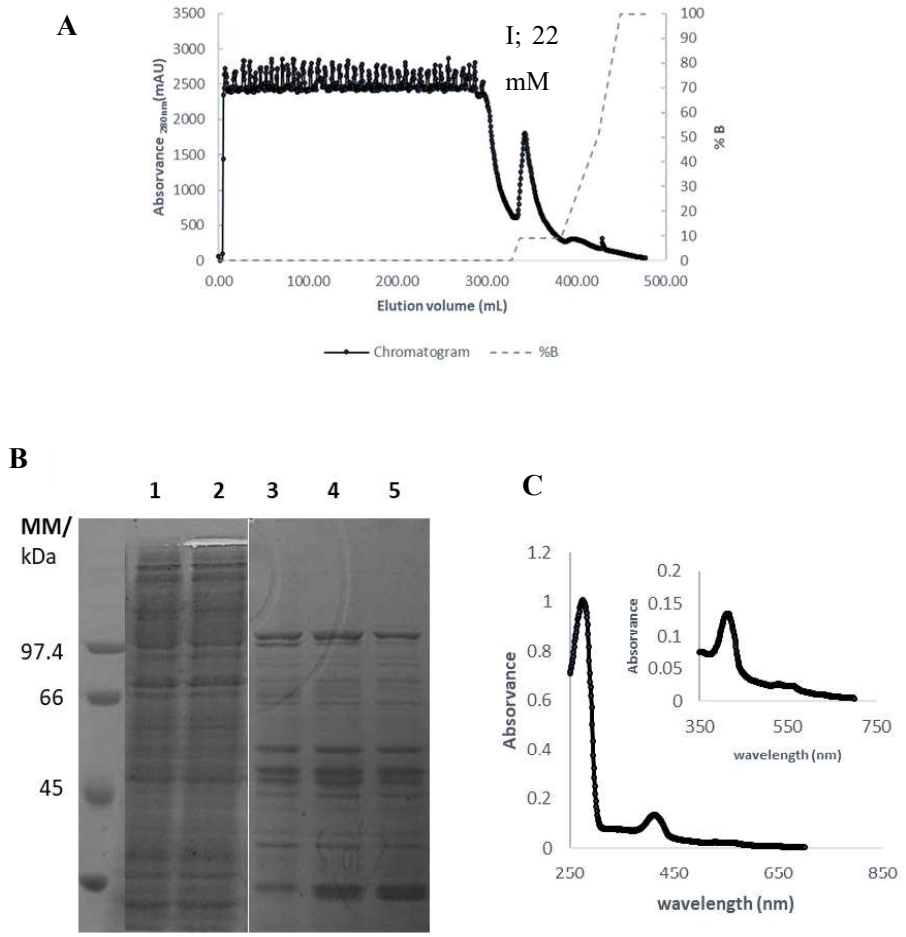

Figure 4.3- **First trial purification of MpsAB-6xHisTag using a HiTRAP charged with nickel.** (A) Chromatogram of the purification in a 5mL HiTRAP nickel charged column, with 50mM KPi pH 7.50, 10 % glycerol, 500 mM NaCl. Flow=5mL/min. (B) SDS-PAGE gel of the purification. Where 1 and 2 are samples corresponding to the fraction that flowthrough the column; and 3 to 5 are samples corresponding to the peak at 22 mM histidine. (C) The UV-spectra of the concentrated samples that correspond to the protein eluted with 22 mM histidine.

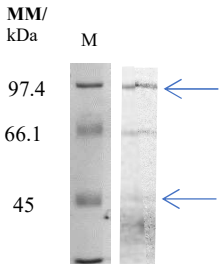

Figure 4.4- **SDS-PAGE gel from the second injection of the purified faction containing the MpsAB-6xHisTag in a HiTRAP**. 12.5% acrylamide SDS-PAGE, the blue arrows represent the samples sent for MS. M: Protein Marker low-range (BioRad)

A new purification strategy should be attempted to purify this complex. Although the protein has a 6xHisTag, purification using a HiTRAP charged with nickel may not be optimal. When performing the purification of proteins with 6xHisTags there are some considerations to account for, *e.g.* "does the 6xHisTag bind strongly to the nickel ions?", "are they available to interact with the chelating ions?" and "are there better chelating ions than nickel?". To address this last question, other ions such as Co^{2+}; Zn^{2+}; Fe^{2+} could be tested [98,99].

4.2 Malate:Quinone Oxidoreductase from *Staphylococcus aureus*

MQOs are FAD-dependent membrane-associated enzymes that catalyze the oxidation of malate to oxaloacetate and donate the electrons to quinones in the ETC [26,28,30,31,34].

S. aureus encodes two putative MQOs, mqoI and mqoII respectively. Although the genes were annotated as coding for mqos, a recent work showed that the second gene copy actually encodes a lactate:quinone oxidoreductase [77,80].

Since 1969 [82] it is known that *S. aureus* could metabolize lactate in a NAD-independent manner but no gene clusters coding for this enzyme were found in its genome.

4.2.1 Malate:quinone oxidoreductase I

4.2.1.1 Protein Purification

Three purification trials were performed to obtain the MQOI, changing the buffer solution and chromatographic procedures (different chelants and/ or gradients).

Elution of protein appeared to occur with 11.75 mM *L*-histidine (Figure 4.5a). The eluted fraction was then concentrated using an AMICON 30 kDa and the UV-visible spectrum of the concentrated fraction was obtained.

All the purification trials resulted in a contamination with cytochrome and other proteins. Further optimization of the MQOI purification procedure is still needed.

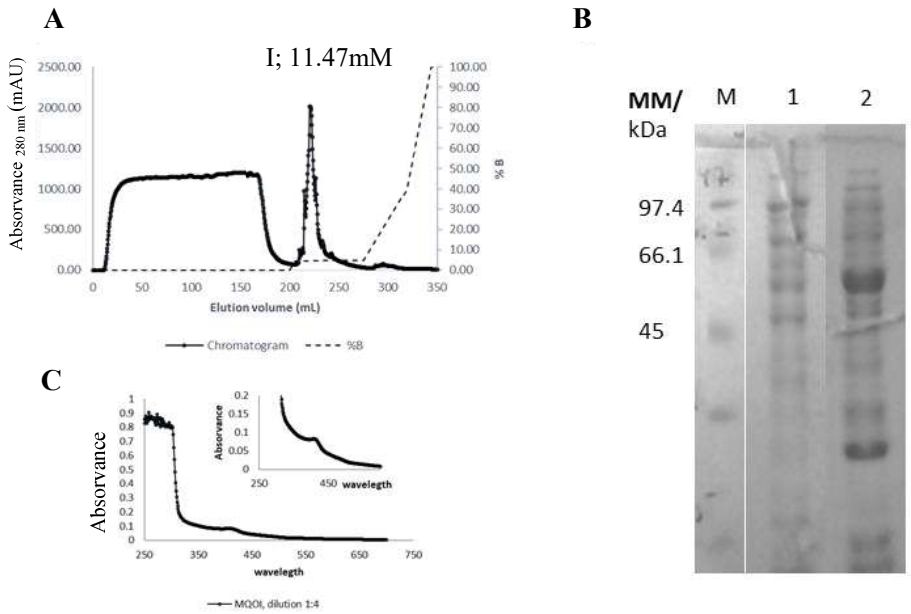

Figure 4.5 **- Purification of MQOI using a HiTRAP charged with nickel. (**A) Chromatogram of the purification in a 5mL HiTRAP nickel charged column, with 50 mM KPi pH 7.00, 10 % glycerol, 300 mM NaCl and a L-histidine gradient (0 to 250 mM). Flow=5mL/min. (B) SDS-PAGE 12.5 % acrylamide gel. Lane: M, low-range marker (BioRad); 1, flow-through of the column; 2, eluted protein with 11.47 mM histidine. It's possible to observe a more intense band below the 66 kDa marker that could correspond to the MQOI protein since it has an expected molecular weigth 57.01 kDa. (C) UV-visible spectra of the concentrated fraction with a dilution factor of 1:4. A peak is visible around 410 nm, which indicates cytochrome contamination [97].

4.2.2 Malate:quinone oxidoreductase II / Lactate:quinone oxidoreductase from *Staphylococcus aureus*

4.2.2.1 Protein purification

To purify this protein four purification trials were attempted but only one resulted in an active protein with flavin content. The successfull chromatographic procedure will be described here.

Since protein precipitation was observed when 2 M NaCl were used to wash the membranes, the subsequent washes were performed with 1 M NaCl. The washed membranes were then solubilized in 1 % (w/w) DDM. The reason to choose DDM to solubilize the membranes is due to the fact that MQOs are described as monotopic proteins with high electrostatic forces and detergents were shown to enhance its activity, as described elsewhere [28-32].

In the chromatogram (Figure 4.6a) after the flowtrough of the column two peaks are presented - one at 162 mL, fraction I, and another at 189 mL, fraction II, eluted at 29 mM and 59 mM histidine respectively. The SDS-PAGE (Figure 4.6b) shows a more intense band at 55 kDa in fraction I, but other bands corresponding to other proteins with different molecular masses are also visible indicating that the fraction is not yet completely purified.

To confirm the presence of the lactate:quinone oxidoreductase in the two fractions after the flowthrough, enzymatic studies following the reduction of DCPIP at 600 nm were performed using a potassium lactate solution as an electron donor at 25 °C. DCPIP is an artificial electron acceptor that upon reduction changes colour allowing its monitorization spectrophotometrically. This compound is commonly used in biochemical studies of ETC enzymes. So, if MQOII is present in the sample it will catalyse the oxidation of lactate with the reduction of DCPIP. The fraction eluted at 14.5 % B (29 mM Histidine) presented a higher activity compared to the other fractions (Table 4.2), the existence of activity in the flowthrough could either be indicative that some overexpressed protein did not chelate with the zinc ion or due to the activity of the iLDH from *E. coli* [100].

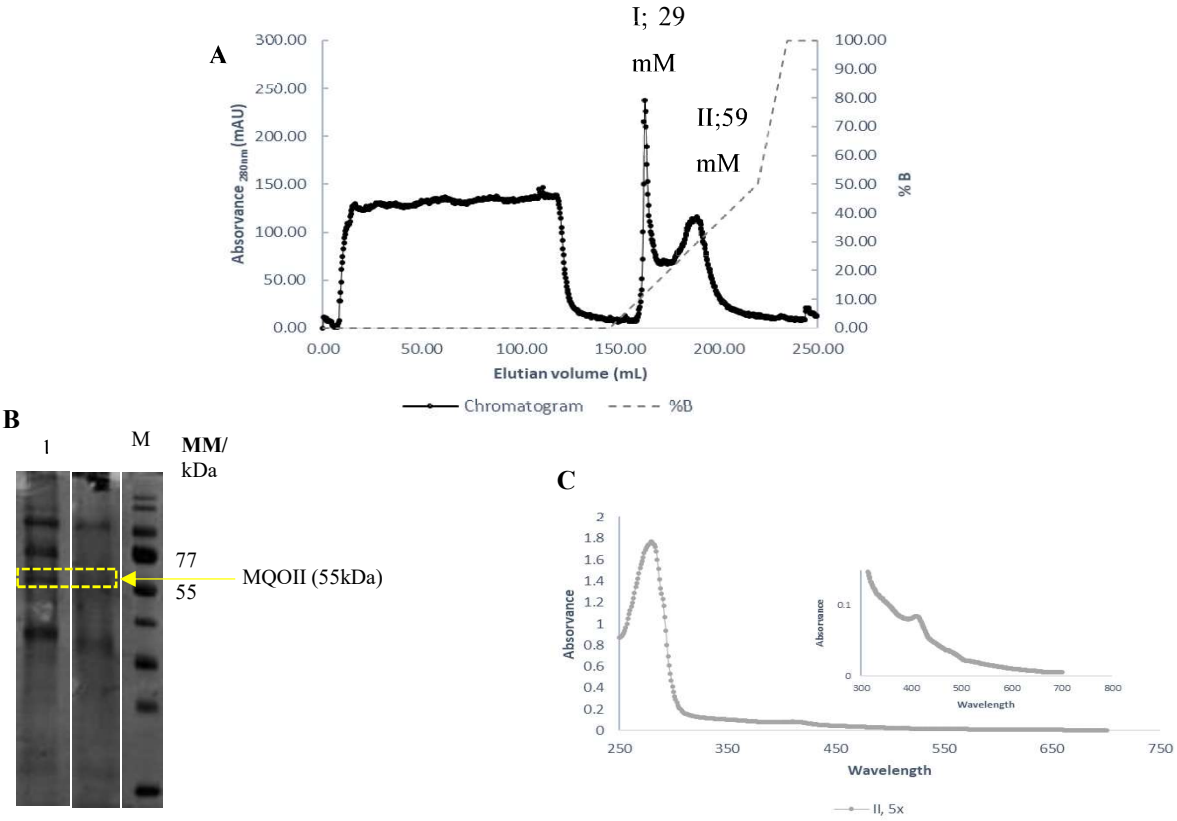

Figure 4.6- **Purification attempt of MQOII using a HiTRAP charged with zinc.** (A) Chromatogram of the purification in a HiTRAP 5mL column zinc charged, with 50 mM KPi pH 7.0, 10 % glycerol, 300 mM NaCl and a *L*-histidine gradient (0 to 200 mM). Flow=5mL/min. (B) SDS-PAGE 12.5 % acrylamide gel. Lane: M, peqGold Protein Marker IV (VWR); 1, eluted protein with 28 mM histidine concentrated with an Amicon 30 kDa. A band corresponding to 55 kDa is visible possibly corresponding to the purified protein, 2; Eluted protein with 59 mM histidine, concentrated with an Amicon 30 kDa (C) UV-visible spectra of the concentrated fraction after a 5-fold dilution. A peak is visible around 410 nm, possibly corresponding to cytochrome contamination [97].

Table 4.2 – **Purification of MQOII using a HiTRAP charged with zinc**

Fraction	Total Protein	Enzymatic Activity [a]
	mg	µmol.sec^{-1}.mg^{-1}
Flowthrough	0.079	4.06
I	0.136	8.20
II	0.422	0.72

[a] Activity calculated using the total amount of protein

The biochemical parameters for *L*-lactate were calculated. The apparent K_m and V_{max} calculated were respectively 40 ± 10 mM and 5000 ± 1214 nmol.min^{-1}.mg^{-1} (calculated from Figure 4.7). Due to the relatively low value of K_m it is suspected that this enzyme has an affinity for the substrate.

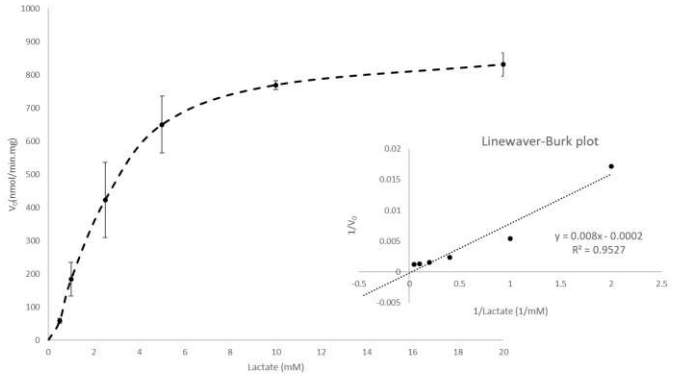

Figure 4.7- **Biochemical study of MQOII from *S. aureus***. Kinetic parameters of MQOII were obtained by varying the concentration of L-lactate. A Lineweaver-Burke plot is shown in the inset. The calculated K_m is 40 ± 10 mM while V_{max} is 5000 ± 1214 nmol.sec^{-1}.mg^{-1}. Data are shown as mean values ± SE of three biologic replicates.

Other assays were performed in the presence of 100 µM and 50 µM of HQNO, to confirm that the enzymatic activity measured was in fact due to MQOII. HQNO is a quinolone and is described as being a potent inhibitor for quinone interaction enzymes.

While the presence of 50 µM HQNO results in almost no inhibition of DCPIP reduction, 100 µM HQNO results in an almost complete inhibition of DCPIP reduction (Figure 4.8). This allows the confirmation that the measured DCPIP reduction is due to the activity of a quinone oxidoreductase.

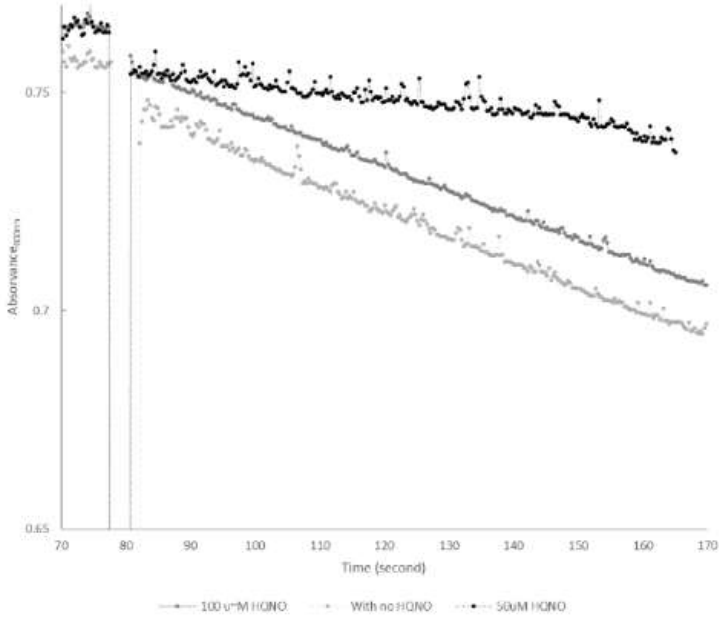

Figure 4.8- **Behaviour of the purified enzyme in the presence of HQNO**. When 100 µM of HQNO is present in the sample an almost complete enzymatic inhibition is seen (dark grey) in comparison when no HNQO is present (light grey). When only 50 µM of HQNO are present almost no effects are observed in the reduction of DCPIP.

Although kinetic parameters of MQOII were determined for *L*-lactate using DCPIP as the electron acceptor, there is still much work left to achieve a better understanding of this enzyme. For instance, the inhibitory constant of HQNO for this condition is not known. Also, the study of this enzyme should also be made using a quinone analogue as an electron acceptor; this way the results obtained will be physiologically more significant.

4.3 The impact of MQOI and MQOII in the energetic metabolic metabolism of *Staphylococcus aureus*

The enzyme MQOI is an important enzyme of *S. aureus* since it can link two important metabolic pathways: the TCA cycle with ETCs. The MQOII is also an important enzyme for the ECTs of *S. aureus*. This pathogenic bacterium is responsible for millions of deaths worldwide[49], but little is known about its respiratory system – which could be a possible target for treatment of infection.
To understand how these monotopic enzymes affect the metabolism of *S. aureus*, growths of different strains were performed in CDM with different carbon sources. Three strains where used, a wild-type strain and two transposon strains that contain a transposon on each gene coding for the MQOs.

4.3.1. The need for riboflavin

Riboflavin is a micronutrient important for all life forms since it is the precursor of two important cofactors of many flavoproteins involved in the cellular metabolism. One such cofactor is synthesized through the phosphorylation of riboflavin resulting in the production of FMN. If followed by the transference of an adenylyl group the formation of FAD occurs [101].
A study using sequence alignment and analysis suggests that some *S. aureus* strains are auxotrophic for riboflavin [102]: not only do they possess a riboflavin biosynthesis pathway (RBP) but, as many other bacteria, they also contain a gene encoding for a riboflavin importer [103] that can uptake the riboflavin from the medium.
It is hypothesized that some RBP containing bacteria also conserve riboflavin transporters due to the fact it can represent an advantageous way of riboflavin acquisition. This hypothesis was suggested since riboflavin uptake using transporters requires less energy in comparison with endogenous biosynthesis [104].
The first chemical defined medium (CDM) used in this work was based on the work of Vikto *et. al* [91] and Patte *et. al* [92] in which the medium does not contain riboflavin. However, in the work of Hussain *et. al* [93] a very similar medium is described but supplemented with this micronutrient.

To understand the importance of riboflavin in the metabolism of *S. aureus* JE2 wild-type (WT) a growth comparison was made in CDMG containing riboflavin and in a CDMG without riboflavin (Figure 4.9). When riboflavin was present growth improvement was observed and the cells reached higher OD_{600nm}.

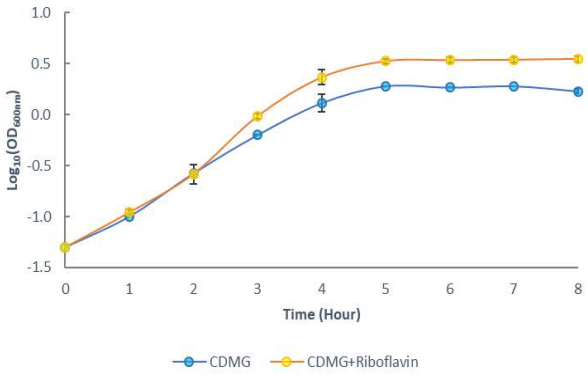

Figure 4.9- **Growth comparison of the WT strain in CDMG containing riboflavin and a non-containing CDMG.** WT growth in a defined media with riboflavin (yellow line) and without riboflavin (blue line) are presented. The growth was made at 37 °C, 200 rpms with a liquid-to-air volume of 1:10. Data are shown as median values ± SE of three biologic replicates. When riboflavin is present the final OD_{600nm} is higher in comparison with without riboflavin.

With this result in mind all the following growths of *S. aureus* were made in the presence of riboflavin.

4.3.2 *Staphylococcus aureus* growth profile on different carbon sources

S. aureus is a facultative anaerobe capable of performing cellular respiration in the presence of an electron acceptor or, in its absence, carbohydrate fermentation. The high adaptive capacity of this pathogen is due to its robust metabolism, that allows for its growth in various environmental conditions [57,62,105].

To try to understand how the MQOI and MQOII can be important for *S. aureus* metabolism, transposon strains with the insertion of erythromycin resistance marker in *mqoI* and *mqoII*, SAUSA300_2541 and SAUSA300_2312 respectively, were studied when grown on different carbon sources.

S. aureus metabolism is described as having two metabolic states. In the first metabolic state an incomplete oxidation of rapidly catabolized metabolites occurs, e.g. glucose [106] and serine, to produce pyruvic acid, during the exponential phase[62]. During this phase, the TCA cycle is repressed. The catabolite control protein A (CcpA) is a transcriptional regulator controlling carbon-metabolism pathways that regulates the use of preferred carbon sources over secondary ones. During the exponential phase, as mentioned, CcpA represses the TCA cycle through the regulation of the genes and protein associated with it [107]. The second metabolic state is when de-repression of TCA cycle occurs: this happens when the carbon sources are depleted from the medium. [108–110]. So, upon the post-exponential phase, the acetate accumulated is fed to the TCA cycle. To enter the TCA cycle the acetate must first

be converted to acetyl-CoA; this reaction can either be catalysed by phosphotransacetylase/acetate kinase or by the acetyl-CoA synthetase.

When *S. aureus* JE2 wild-type (WT), SAUSA300_2541::Tn (MQOI::Tn) and SAUSA300_2312::Tn (MQOII::Tn) were grown in CDMG (Figure 4.10b) it was possible to observe that during the exponential phase of growth (first 5 hours) a decrease in pH occurs for all strains. This decrease was more pronounced in the WT strain.

This decrease in pH is normally associated with the accumulation of acetate that leads to medium acidification [111]. After the exponential phase it is possible to observe an increase in the measured pH that could reflect the alkalization of the media due to ammonia accumulation [111,112]. This accumulation is the result of the anaplerotic reactions that are required to maintain the TCA cycle functional. Because staphylococci lacks a glyxylate shunt [109,111–113], for every two carbons that enter the TCA cycle as acetyl-CoA two carbons are lost as carbon dioxide. So, if carbons are being withdrawn from the TCA cycle a way of maintaining it is by anaplerotic reactions using amino acids as substrates that will provide TCA cycle intermediates. Prior to entering the TCA cycle, a deamination is required resulting in the accumulation of ammonia in the culture medium.

When comparing the growth curves (Figure 4.10a), the three strains were observed to reach nearly the same OD_{600nm} and the main difference observed between them was in the exponential phase. During the exponential phase the OD_{600nm} observed for the two mutants was lower than the WT. Also, the mutants took a longer time to achieve the post-exponential phase compared to the WT.

In the growth in which lactate (5 mM) was the primary carbon source (Figure 4.11a) the growth curves of MQOI::Tn and MQOII::Tn were very similar. The shape of the growth curves was similar for the three strains, but the WT had an exponential phase with higher OD_{600nm}.

In the pH evaluation (Figure 4.11b), a different pattern was observed for each strain. The WT strain kept the pH constant for about 2 hours followed by a small decrease during 2 hours and then an abrupt pH raise was observed. Both MQOI::Tn and MQOII::Tn also had a raise in pH but while the latter had a drop in pH at the fourth hour of growth, the first one appeared to only raise the pH after the sixth hour of growth.

When the growth medium has acetate, CDMA, (Figure 4.12a) it was observed again that the WT strain achieved a post-exponential phase with higher OD_{600nm} and the growth profiles of the transposon strains were once again very similar between them. The WT strain maintained a stable pH in the first 4 hours of growth and in the following hours an increase in pH was observed (Figure 4.12.b)

The pH variation profiles and growth curve for the transposon strains were very similar between the two.

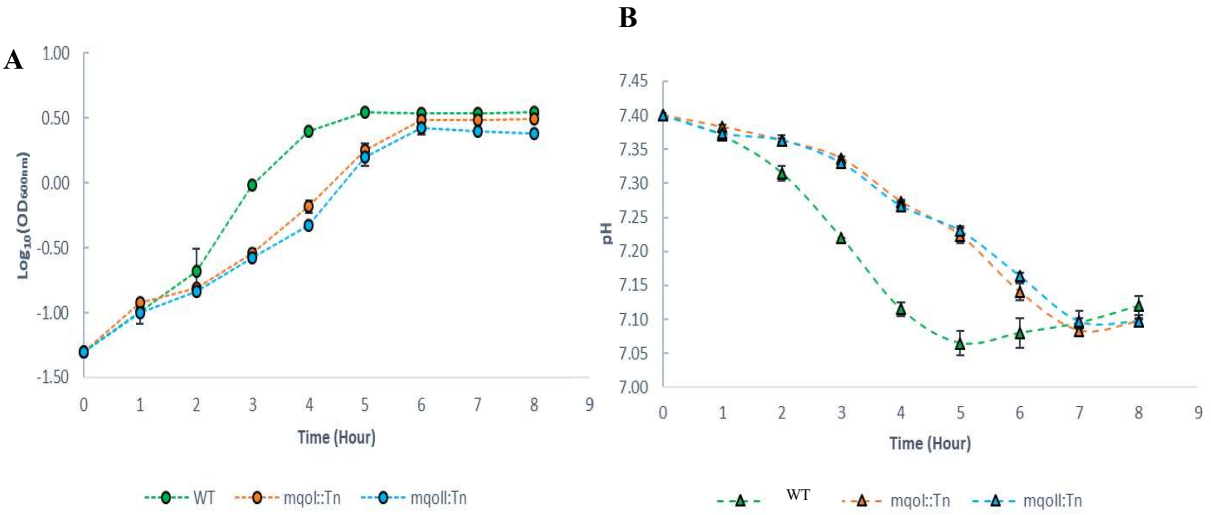

Figure 4.10- **Growth curves and pH evaluation of WT, MQOI::Tn and MQOII::Tn in CDMG.** (A) growth curves of the WT (green circles), MQOI::Tn (orange circles) and MQOII::Tn (blue circles) during 8 hours in CDMG. (B) pH evaluation during 8 hours of growth in CDMG of WT (green triangles); MQOI::Tn (orange triangles) and MQOII::Tn (blue triangles). Data are shown as mean values ± SE of three biologic replicates.

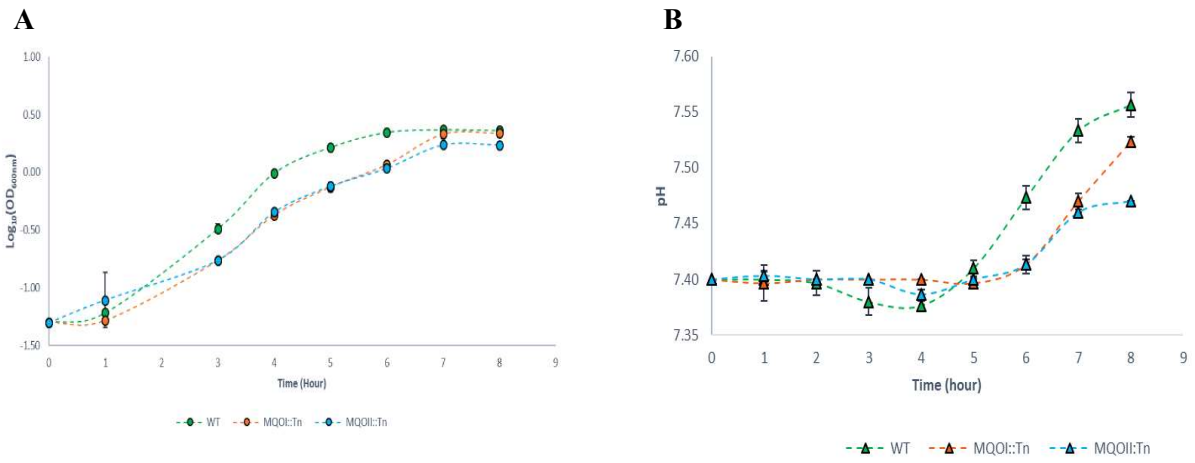

Figure 4.11- **Growth curves and pH evaluation of WT, MQOI::Tn and MQOII::Tn in CDML.** (A) Growth curves of the WT (green circles), MQOI::Tn (orange circles) and MQOII::Tn (blue circles) during 8 hours in CDML. (B) pH evaluation during 8 hours of growth in CDML of WT (green triangles); MQOI::Tn (orange triangles) and MQOII::Tn (blue triangles). Data are shown as mean values ± SE of three biologic replicates.

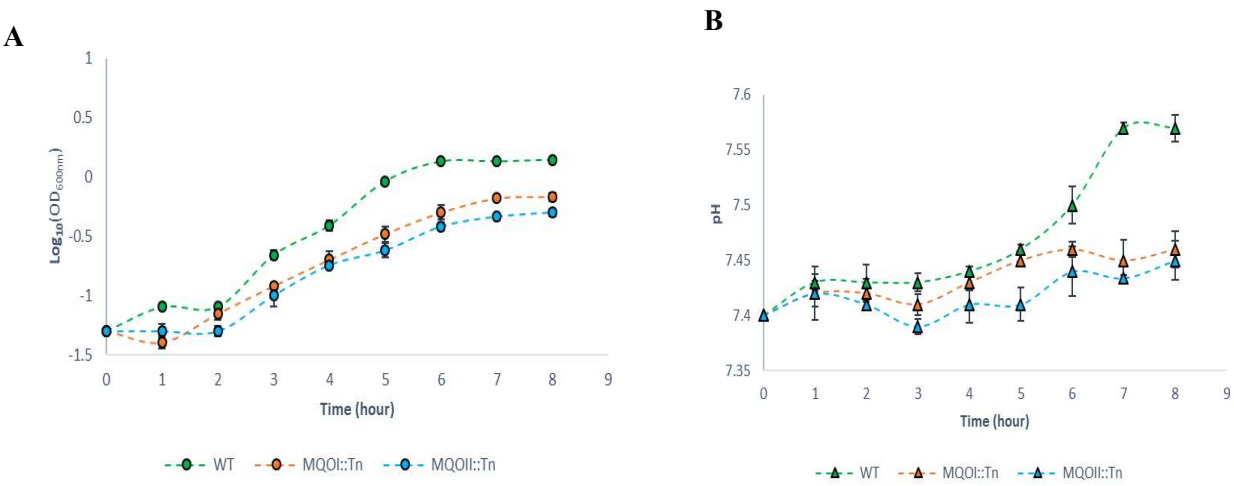

Figure 4.12- **Growth curves and pH evaluation of WT, MQOI::Tn and MQOII::Tn in CDMA.** (A) Growth curves of the WT (green circles), MQOI::Tn (orange circles) and MQOII::Tn (blue circles) during 8 hours in CDML. (B) pH evaluation during 8 hours of growth in CDML of WT (green triangles); MQOI::Tn (orange triangles) and MQOII::Tn (blue triangles). Data are shown as mean values ± SE of three biologic replicates.

For all the three strains studied (WT, MQOI::Tn and MQOII::Tn) glucose was the carbon source that allowed for higher cellular growth followed by lactate and then acetate (Figure 4.13).

The shape of the growth curves for glucose (purple points) and lactate (grey points) are very similar in each strain (Figure 4.13) when compared to the respective growth curves in acetate (red points). In the growth curve with acetate as carbon source it is always observed that the exponential phase takes longer and a lower OD_{600nm} is achieved at the end of the growth.

All this data shows that MQOI and MQOII affect the metabolism of *S. aureus*. It also demonstrates that the two enzymes are not isoenzymes since the loss of expression of one could not be compensated by the expression of the other. The two transposon mutants showed growth defects when compared to the WT.

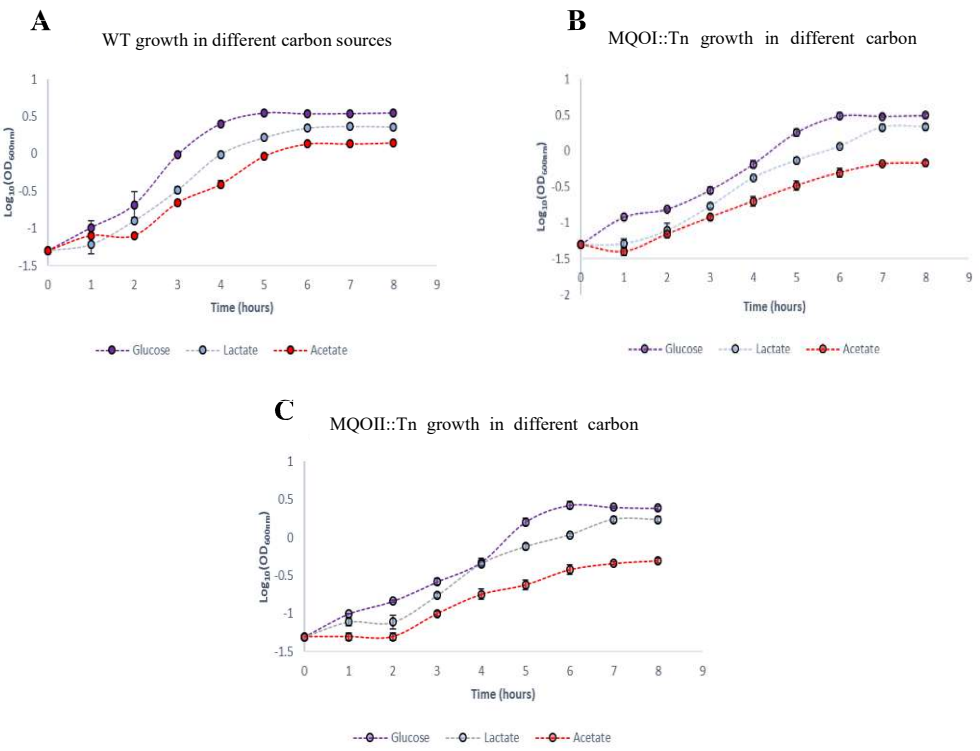

Figure 4.13- **Comparison of the growth curves of WT, MQOI::Tn and MQOII::Tn in different carbon sources.** Carbon source present in the medium glucose (purple dots), lactate (grey dots), acetate (red dots) for (A) growth curves of the WT for 8 hours, (B) MQOI::Tn for 8 hours. (C) Growth curve of MQOII::Tn 8 hours. Data are shown as mean values ± SE of three biologic replicates.

To further explore the metabolic footprint of *S. aureus* a CDMG growth was made and the extracellular metabolic footprint (exometabolome) of each strain was analyzed by NMR.

4.3.3 *Staphylococcus aureus* exometabolomic footprint

S. aureus in comparison with other gram-positive bacteria lacks some metabolic overlap/redundancy [112] but it is still a metabolic robust bacteria. Its capacity to survive the administration of various antibiotics to an infected patient is in part due to the metabolic adaptations that *S. aureus* can undergo [113–115]. Normally, this metabolic adaptation can occur as changes in the central metabolism, which can modify the biosynthetic intermediates availability for the synthesis of macromolecules needed for bacterial survival.[62]

To further investigate how MQOI and MQOII could influence the bacteria physiology, the exometabolome of the WT, MQOI::Tn and MQOII::Tn were investigated.

The ^{1}H-NMR spectroscopy allowed for the analysis of the metabolic footprint[116] during the growth curve of each strain.

By using CDMG with a liquid-to-air rate of 1:5 a well reproducible growth is achieved for all strains, which is reflected by the reproducible exometabolic profiles (Figure 4.14). Using ^{1}H-NMR analysis, it was possible to identify 12 amino acids from the 18 existing in the medium (Figure 4.15). Of the nitrogenous bases only guanine was not identified (Figure S5). The vitamins present in the medium were not quantified since their concentrations were below the detection limit of the analytical method. It was also possible to detect the secretion of metabolites in the supernatant of *S. aureus* WT, MQOI::Tn and MQOII::Tn; in total 21 metabolites were identified and quantified and 2 unidentifiable NMR peaks were visible. But the identification of these unknown metabolites should be performed as they may contribute for a better understanding of *S. aureus* metabolism. (Figure S6**).**

When *S. aureus* is grown in aerobic conditions with an excess of glucose an incomplete oxidation of the carbohydrate occurs, mainly by glycolysis [106], to pyruvate, which is then forced into the overflow metabolism since the TCA cycle in this condition is mainly inactive. The main overflow metabolite produced in this condition is acetate [116–118]. The data obtained was also in agreement with the literature, since the WT accumulated 7.3 mM acetate. The MQOI::Tn and MQOII::Tn accumulated 9 mM acetate (Figure 4.14). Another overflow metabolite, lactate, was also identified for the three strains.

When comparing the secretion concentration of lactate with acetate, lactate was secreted in lower quantities. Although the signals for pyruvate were apparently identified, its quantification was not possible since its signal was overlapped with a signal from glutamic acid and more signals where present in the chemical shift expected for pyruvate (Figure S7).

All the three strains appear to use the overflow metabolism in different proportions which results in different accumulation patterns (Figure 4.14).

Interesting data was observed regarding acetate accumulation. In the WT strain acetate accumulated during 7 hours of growth but at the 8th hour of growth a decrease in acetate concentration occurred, indicating that the TCA cycle was no longer repressed by glucose and uptake of acetate was observed. While MQOI::Tn seems to accumulate acetate until 7 hours of growth but then its concentration is maintained. The MQOII::Tn strain seems to accumulate acetate in the 8 hours of growth.

In WT and MQOI::Tn the lactate was excreted during the exponential phase and was consumed in the post-exponential phase. This behaviour is in agreement with data observed in the literature for the WT strains studied [116,118]. MQOII::Tn is apparently unable to metabolize the accumulated lactate.

The minimal accumulation of TCA cycle intermediates in the supernatant could indicate that either the TCA cycle is not fully repressed, but that its activity is only decreased; or that accumulation of TCA cycle intermediates is due to the amino acid metabolism.

From the 13 amino acids identified all the strains fully consumed aspartate, glutamate acid, alanine and glycine (Figure 4.15). Phenylalanine, threonine, methionine, tyrosine, and valine were not fully consumed. In the group of amino acids that were not completely consumed, the consumption of methionine and valine appeared to occur to a higher extension than the others.

A difference was visible in the uptake of histidine between the WT and the two transposon strains: while the first fully consumed histidine, the transposon strains appeared to have an impairment in histidine uptake.

While the MQOII::Tn strain did not fully consume isoleucine the WT and MQOI::Tn strains fully consumed that amino acid.

The cystine uptake pattern was also different between the MQOII::Tn strain and the other two, since it fully consumed cystine while the WT and MQOI::Tn did not (Figure 4.15)

An interesting finding was ethanol production in the WT, although its concentration was below 0.5 mM (Figure 4.16). This could indicate that when a liquid-to-air volume of 1:5 is used *S. aureus* may not be in a full aerobic condition. For the transposon strains ethanol was present in the medium due to the preparation of erythromycin, and it is possible that to a low extent the ethanol present is being metabolized, since a decrease in its concentration is observed (Figure S8).

When accomplishing the identification and quantification of lactate, cystine and threonine, it was observed that both ^{1}H-NMR signals from lactate overlapped with signals from cystine and threonine which have the same shape. At 4.1 ppm lactate has a quadruplet – cystine has a quadruplet at the same chemical shift; at 1.2 ppm lactate has a doublet – threonine has a doublet at this same chemical shift. Even so, the quantification of cystine and threonine was achieved by using other signature spectra areas and lactate was identified since over the growth time samples the shape of the quadruplet gradually changed (Figure S9).

Since threonine is not fully consumed, a growth without it should be tried in the future to understand how it is affected. If the growth stays unaffected then a ^{1}H-NMR exometabolome should be performed. This way a more precise quantitation of lactate could be achieved.

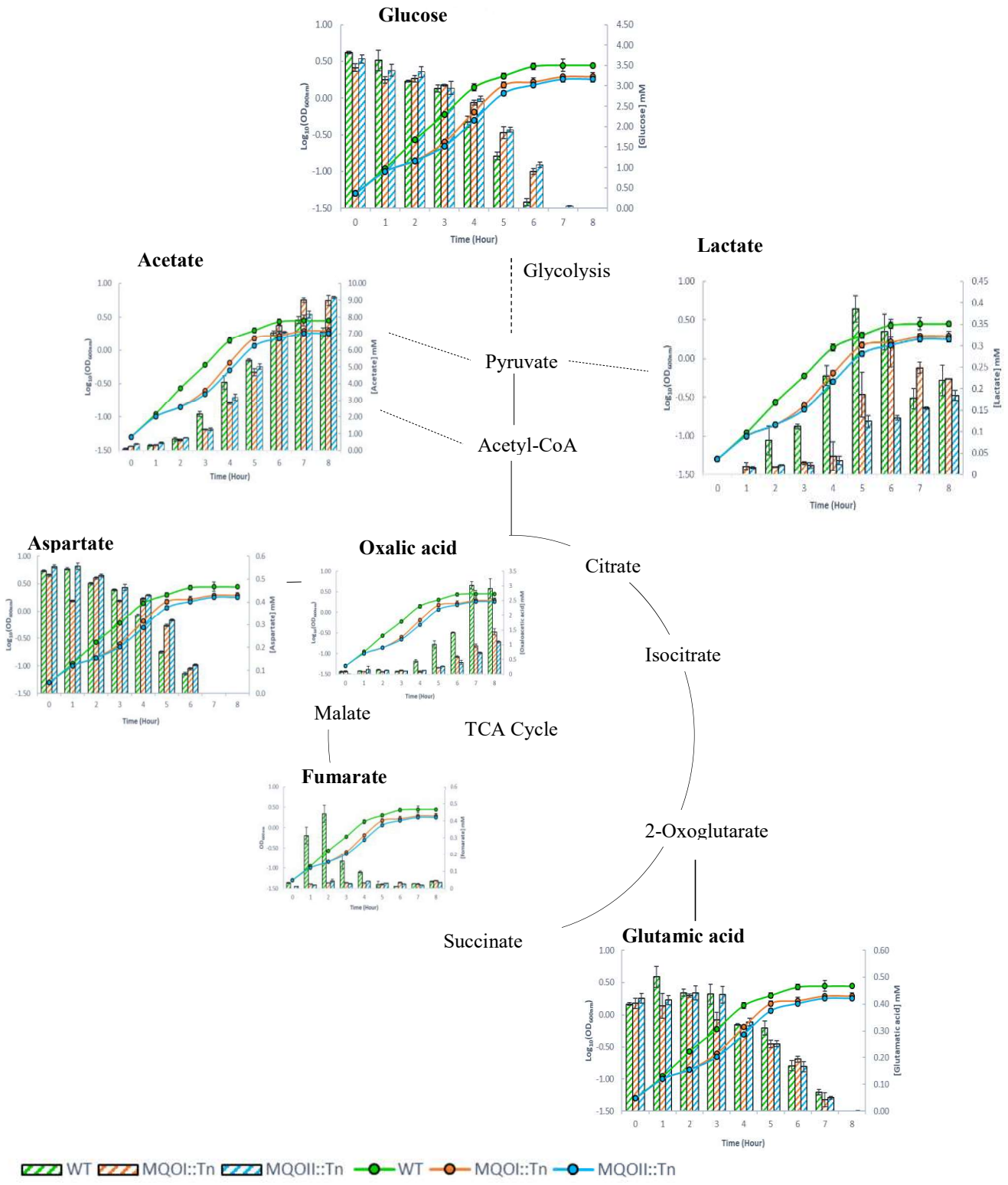

Figure 4.14- **Overflow metabolites and associated metabolic pathways**. Time-resolved extracellular metabolite concentration of WT (green), MQOI::Tn (orange) and MQOII::Tn (blue) are arranged according to their intracellular metabolic pathways: glycolysis, pyruvate metabolism, TCA cycle and glutamate metabolism. Dashed lines represent multiple successive enzymatic reactions. Data are shown as mean values± SE of three biological samples.

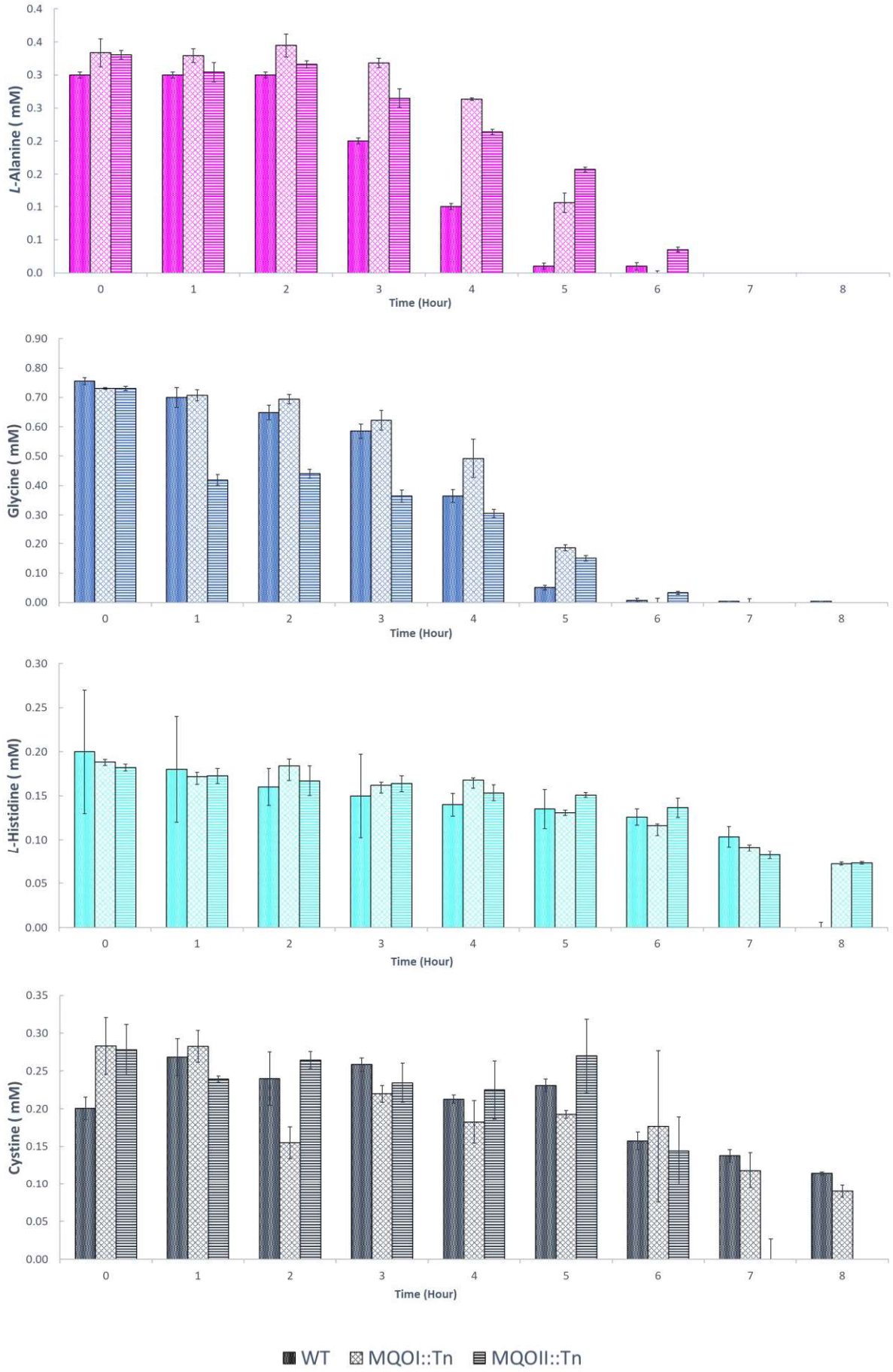
L-Alanine (mM)
Time (Hour)
Glycine (mM)
Time (Hour)
L-Histidine (mM)
Time (Hour)
Cystine (mM)
Time (Hour)
WT
MQOI::Tn
MQOII::Tn

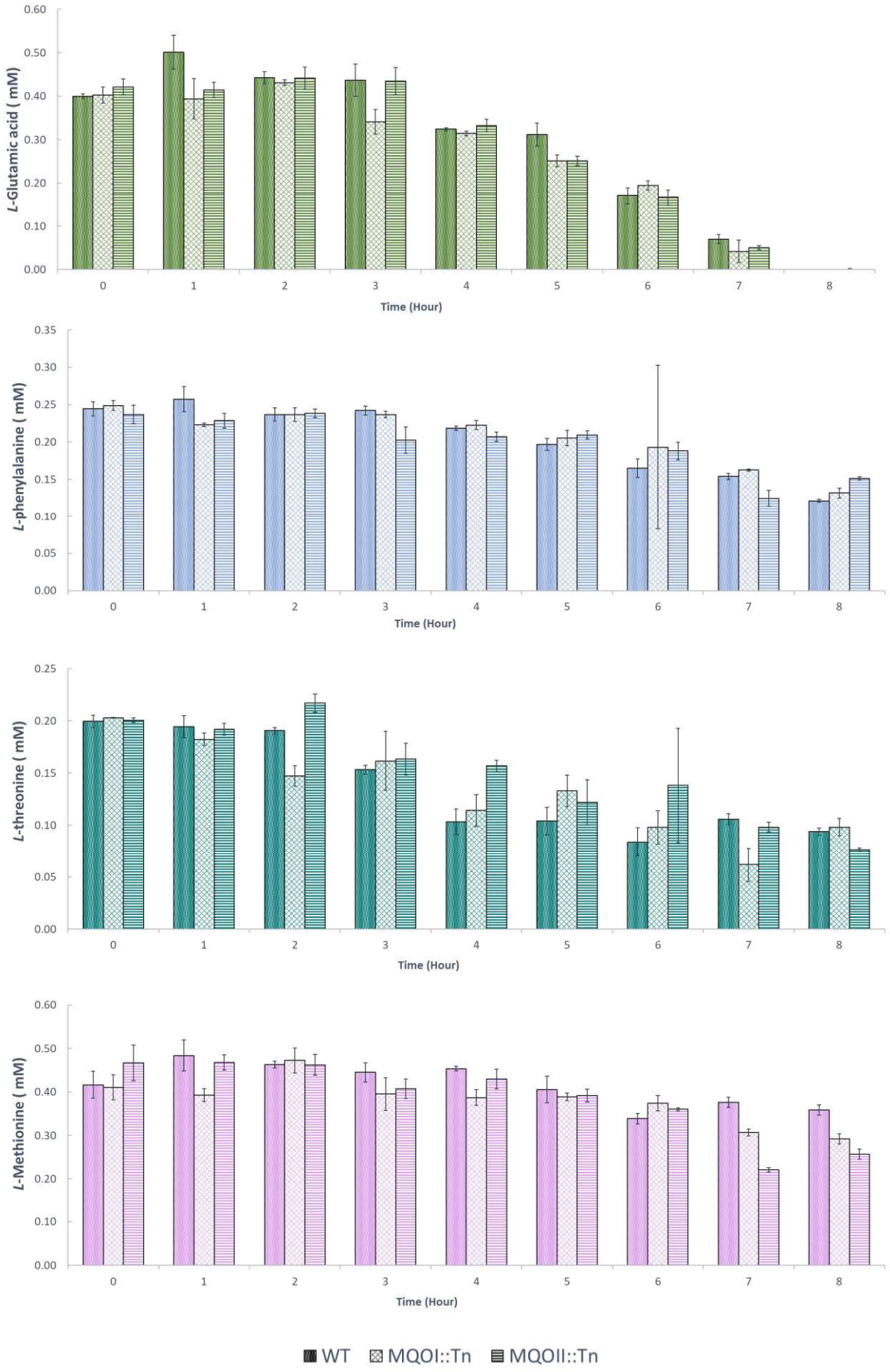
L-Glutamic acid (mM)
0.60
0.50
0.40
0.30
0.20
0.10
0.00
0 1 2 3 4 5 6 7 8
Time (Hour)
L-phenylalanine (mM)
0.35
0.30
0.25
0.20
0.15
0.10
0.05
0.00
0 1 2 3 4 5 6 7 8
Time (Hour)
L-threonine (mM)
0.25
0.20
0.15
0.10
0.05
0.00
0 1 2 3 4 5 6 7 8
Time (Hour)
L-Methionine (mM)
0.60
0.50
0.40
0.30
0.20
0.10
0.00
0 1 2 3 4 5 6 7 8
Time (Hour)
WT
MQOI::Tn
MQOII::Tn

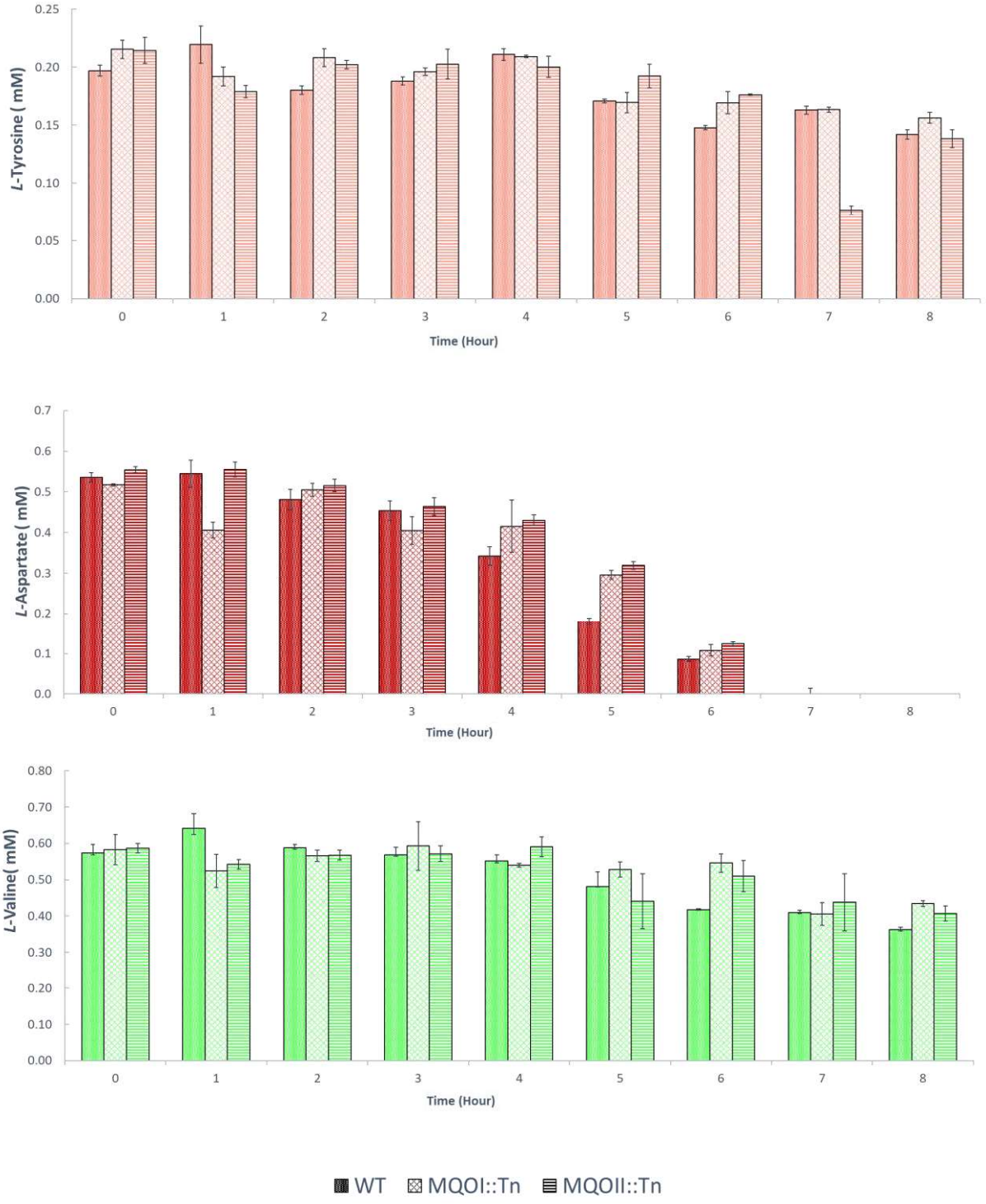

Figure 4.15- **Amino acid uptake pattern for WT, MQOI::Tn and MQOII::Tn strains.** Time-resolved extracellular amino acid concentration for WT, MQOI::Tn and MQOII::Tn. The data represent the mean ±SE values for biological triplicates.

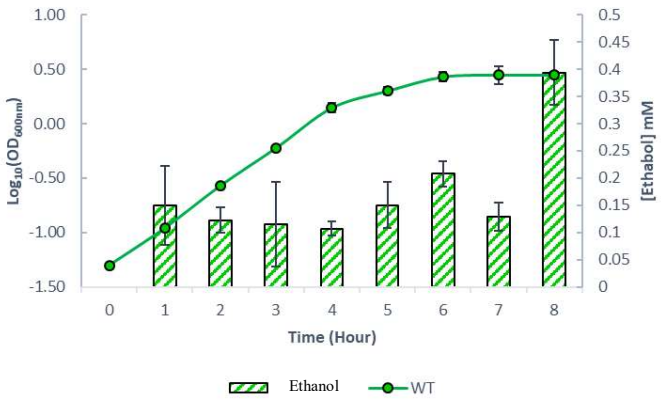

Figure 4.16- **Ethanol production by WT strain.** Extracellular ethanol concentration for the WT strain. The data represented are mean values ±SE values from three biological replicates.

A growth with an air-to-liquid ratio of 1:10 should be made to compare the exometabolome of both growths with different air-to-liquid ratios, since the uptake and secretion pattern of some metabolites may differ.The observation of ethanol production with an air-to-liquid ratio of 1:5 could mean that a full aerobic condition was not achieved. So, it will be interesting to understand how different oxygen concentrations will influence the production of TCA cycle intermediates. As explained before, this pathogen has a highly adaptive metabolism.

Another interesting study to perform is the study of the exometabolome when lactate or acetate is the only carbon source present in the medium, to understand how the central metabolism is affected and how the transposon strains would adapt to such conditions.

4.3.3 Promoter fusion strategy

Aiming to understand in which conditions the MQOs genes of *S. aureus* are activated, a promoter fusion strategy was designed. Therefore, a GFP gene was fused with each promoter region at 5' end. The desired constructs were identified by colony PCR and by diagnostic restriction digestion (Figure 4.17). Having obtained pSP64E+mqoI_GFP and pSP64E+mqoII_GFP plasmids, confirmation that the clone sequence is without errors is still needed and the sequence needs to be determined.

Two *S. aureus* mutants may be achieved by molecular biology techniques where in the genome the wild-type promoter for each MQO would be replaced by the promoter fused with GFP, *mqoI+sGFP,* and *mqoII+sGFP* for each. These new mutants would allow to observe, by fluorescent microscopy, in which growth phase each gene is active and if the activation pattern can change with different carbon sources.

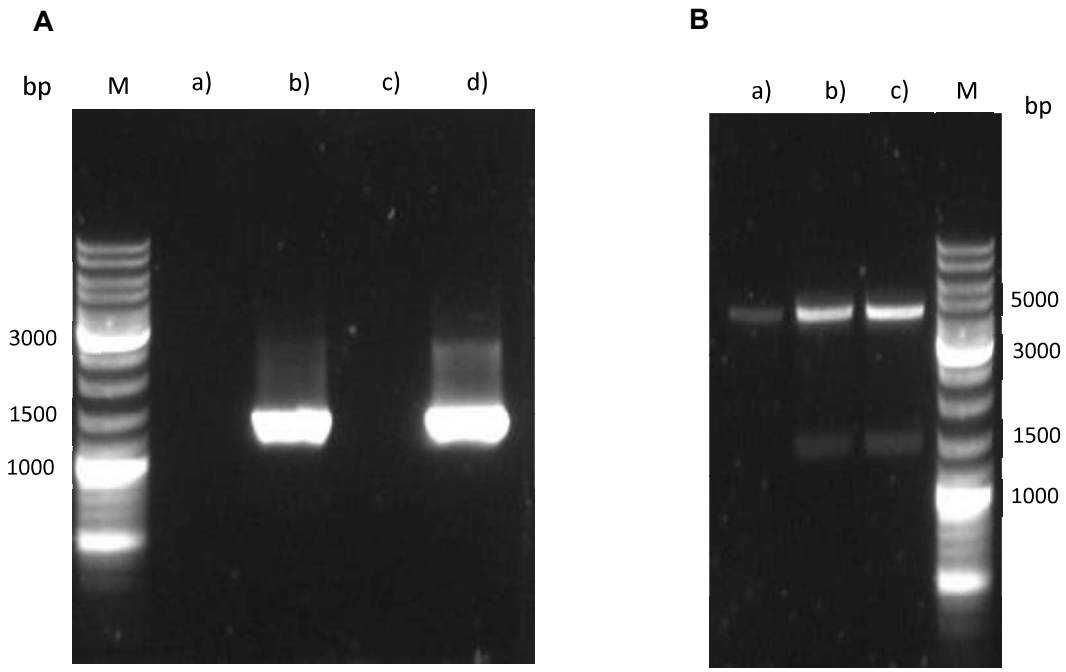

Figure 4.17- **Analysis of the obtained constructs.** (A) Colony PCR results to confirm the presence of the constructed pSP64E plasmid; a) DC10B cells containing the pSP64E plasmid and b) selected colony with the pSP64E+mqoII_GFP plasmid, PCR made with P1-UpMQO2312-EcoRI and P4-sGFP bward XamI; c) DC10B cells containing the pSP64E plasmid d)selected colony with the pSP64E+mqoI_GFP plasmid , PCR made using P1-UpMqo2541-EcoRI and P4-sGFP bwar XmaI; M) GeneRuler DNA Ladder mix(ThermoFisher) (B) Diagnostic restriction digestion; a) pSP64E plasmid digested with EcoRI and XmaI; b) pSP64E+mqoII_GFP digested with EcoRI and XmaI and c) pSP64E+mqoI_GFP digested with EcoRI and XmaI; M) GeneRuler DNA Ladder mix (ThermoFisher). In the colony PCR as well as in the diagnostic restriction digestion it is possible to observe a fragment with 1500 bp that corresponded to the promoter fused with the GFP.

5. Conclusion

Staphylococcus aureus is an opportunist pathogen responsible for a wide variety of clinical manifestations[112,119,120]. It is also a pathogen with high adaptive ability. So, it is important to perform studies that allow a better knowledge of its metabolism - this would allow to understand how *S. aureus* is capable of thriving in many different environmental conditions. This knowledge could then result in the production of new and improved medicines.

Three respiratory enzymes were the focus of this thesis: the MpsAB, MQOI and MQOII. The MQOI is also an enzyme involved in the TCA cycle.

The MpsAB is hypothesized to be involved in the generation of a membrane potential in *S. aureus.* For a better understanding of this enzyme, attempts to isolate it were performed. In this way several expression tests were performed in which different conditions were shown to be promising for the expression of the complex. From those promising conditions the one that allowed its expression with higher biomass production was chosen. A purification trial was performed, but the complex was not isolated. Much work is still needed to achieve the purification of this enzyme and other purification procedures should be attempted. Regarding its expression, instead of heterologous, a homologous expression strategy could also be tested, to observe if expression is enhanced.

For the other proteins studied in this work, several purifications were attempted but only the purification of MQOII was achieved. Although with some contaminants, it was possible to perform some preliminary biochemical characterization, like estimating Km and V_{max}. Biochemical assays performed in the presence of HQNO confirmed that the enzymatic activity was due to a quinone reductase. For a more precise identification mass spectroscopy should have been performed. In this thesis, the enzymatic activities were measured using an artificial electron acceptor but for a more physiologically relevant assay a quinone analogue, *e.g.* 2,3-dimethoxy-5-methyl-1,4-napthoquinone (DMN), should be used. With this strategy it should be possible to calculate the K_m and V_{max} for the two substrates used by the enzyme (*L*-lactate and the quinone), Also, different purification procedures should be attempted for MQOI.

Cellular studies using different carbon sources (glucose, lactate and acetate) have shown that both MQOI and MQOII are important enzymes for the metabolism of *S. aureus*. In all the different growths the transposon strains always showed a delay in growth and lower cell mass production in comparison to the WT. This shows that one enzyme cannot make up for the absence of the other, implying the importance of the two enzymes and as they are not isoenzymes.

Metabolic footprint analysis of the extracellular medium during an eight hour growth of the three strains, WT, MQOI::Tn and MQOII::Tn, done in a chemical define medium was presented. Different metabolic uptake and secretion patterns for the three strains were observed. It appeared that MQOII::Tn is incapable of re-uptake of the excreted lactate.

In the amino acid uptake pattern some interesting findings were observed, as histidine is fully consumed in the WT strain but not in the transposon strains; histidine metabolism results in *L*-aspartate production which can be further metabolized into 2-oxoglutarate (a TCA intermediate). Isoleucine uptake also appears to be impaired in the MQOII::Tn strain in comparison with both WT and MQOI::Tn where it is fully consumed. The other amino acid that gave different uptake patterns was cystine where the MQOII::Tn strain fully consumes it while the other two do not fully consume it.

Ethanol production was detected in the WT strain, which could mean that the cells are not in full aerobic conditions.

Further metabolic footprint assays should be done with different carbon sources (e.g. lactate and acetate) and an air-to-liquid ratio of 1:10 for comparison with the present results. These comparisons would provide more knowledge of the metabolic pathways activated for different carbon sources and oxygen concentrations.

For the future, more precise identification of excreted metabolites could be done, for this, standard solutions of the intended metabolites should be prepared, and their ^{1}H-NMR spectra used to compare the chemical in order to perform their identification.

An intra-cellular metabolic footprint could also represent an interesting study to perform since more information could be gathered about staphylococci metabolism.

By the end of the work, two plasmids, containing the promoters of *mqoI* and *mqoII* fused with a *gfp* named pSP64E+mqoI_GFP and pSP64E+mqoII_GFP respectively, were obtained. These will allow the understanding of when each of the *mqos* are active during an aerobic growth or if *mqos* have any implications for *S. aureus* when strains are grown in different carbon sources.

The absence of either MQOI or MQOII provoked an impaired growth when comparing with WT. Our data showed that both metabolic enzymes were important for the *S. aureus* metabolism and since in Humans there is no enzyme with sequence homology to these proteins [26,77,80] both enzymes could be suitable for new drug therapies in the future.

6. Bibliography

1. Marreiros, B. C. *et al*. Exploring membrane respiratory chains. *Biochimica Biophysica. Acta (BBA) - Bioenerg*etics **1857**, 1857 (2016). doi:10.1016/j.bbabio.2016.03.028

2. Nelson, D. & Cox, M. M. Glycolysis, Gluconeogenesis, and the Pentose Phosphate Pathway. in *Principles of Biochemistry*, 4th edition 521–556 (2004).

3. Nicholls, D. G. & Ferguson, S. J. Respiratory Chains. in *Bioenergetics*, 4th edition 89–136 (Academic Press, 2013).

4. Mitchell, P. Protonmotive redox mechanisms of cytochrome bc_1 complex in the respiratory chain: protonmotive ubiquinone cycle. *FEBS Letters*. **56**, 1–6 (1975). doi:10.1016/0014-5793(75)80098-6

5. Mitchell, P. The protonmotive Q cycle: A general formulation. *FEBS Letters*. **59**, 137–139 (1975). doi: 10.1016/0014-5793(75)80359-0

6. Mitchell, P. Coupling of phosphorylation to electron and hydrogen transfer by a chemi-osmotic type of mechanism. *Nature* **191**, 144–148 (1961). doi: 10.1038/191144a0

7. Tortora, J. G., Funke, R. B. & Case, L. C. Microbial Metabolism. in *Microbiology: An introduction*, 11th edition 112–133 (Pearson, 2012).

8. Lodish, H. *et al*. Biochemical Energetics. in *Molecular Cell Biology*. 5th edition, 50–51 (W. H. Freeman, 2003).

9. Bren, A. *et al*. Glucose becomes one of the worst carbon sources for *E. coli* on poor nitrogen sources due to suboptimal levels of cAMP. *Scientific Reports* **6**, (2016). doi: 10.1038/srep24834

10. Dimroth, P. *et al.* Crucial role of the membrane potential for ATP synthesis by F(1)F(o) ATP synthases. *The Journal of experimental biology* **203** Pt1, 51–9 (2000).

11. Berg, J *et al*. Glycolysis and Gluconeogenesis; The Citric Acid Cycle; Oxidative Phosphorylation. in *Biochemistry*. 5th edition 602-655; 664-695; 700-744 (2002).

12. Stincone *et al*. The return of metabolism: biochemistry and physiology of the pentose phosphate pathway. *Biological Reviews* **90**, 927–963 (2014). doi: 10.1111/brv.12140

13. Chen, X. *et al*. The Entner–Doudoroff pathway is an overlooked glycolytic route in cyanobacteria and plants. *Proceedings of the National Academy of Sciences* **113**, 5441–5446 (2016). doi: 10.1073/pnas.1521916113

14. Krebs, H. A. The citric acid cycle. *Biochemical Journal* **34,** 460–463 (1940). doi: 10.1042/bj0340460

15. Nakano, M. M *et al.* Characterization of anaerobic fermentative growth of *Bacillus subtilis*: Identification of fermentation end products and genes required for growth. *Journal of Bacteriology* **179**, 6749–6755 (1997). doi: 10.1128/jb.179.21.6749-6755.1997

16. Schreiber, K. *et al*. The anaerobic regulatory network required for *Pseudomonas aeruginosa* nitrate respiration. *Journal of Bacteriology* **189**, 4310–4314 (2007). doi: 10.1128/jb.00240-07

17. Sigalevich, P. *et al*. Sulfate reduction and possible aerobic metabolism of the sulfate-reducing bacterium *Desulfovibrio oxyclinae* in a chemostat coculture with *Marinobacter* sp. strain MB under exposure to increasing oxygen concentrations. *Applied and Environmental Microbiology* **66**, 5013–5018 (2000). doi: 10.1128/aem.66.11.5013-5018.2000

18. Wainio, W.W. The respiratory chain. in *The mammalian Mitochondrial respiratory chain* 77-151. (Academic Press,1970). doi: 10.1016/b978-0-12-730650-6.50006-4

19. Efremov, R. *et al.* The architecture of respiratory complex I. *Nature* **465**, 441–445 (2010). doi: 10.1038/nature09066

20. Baradaran, R. *et al*. Crystal structure of the entire respiratory complex I. *Nature* **494**, 443–448 (2013). doi: 10.1038/nature11871

21. Hirst, J. Mitochondrial complex I. *Annual Review of Biochemistry* **82**, 551–575 (2013). doi: 10.1146/annurev-biochem-070511-103700

22. Efremov, R. *et al.* Structure of the membrane domain of respiratory complex I. *Nature* **476**, 414–421 (2011). doi:10.1038/nature10330

23. Lancaster, C. R. Succinate:quinone oxidoreductases: an overview. *Biochimica Biophysica Acta (BBA)***1553**, 1–6 (2002). doi: 10.1016/S0005-2728(01)00240-7

24. Crofts, A. R. *et al*. Pathways for proton release during ubihydroquinone oxidation by the bc_1 complex. *Proceedings of the National Academy of Sciences* **96**, 10021–10026 (1999). doi: 10.1073/pnas.96.18.10021

25. Brandt, U. Energy conservation by bifurcated electron-transfer in the cytochrome bc_1 complex. *Biochimica et Biophysica Acta (BBA) - Bioenergetics* **1275**, 41–46 (1996). doi: 10.1016/0005-2728(96)00048-5

26. Hartuti, E. D. *et al*. Biochemical studies of membrane bound *Plasmodium falciparum* mitochondrial *L*-malate:quinone oxidoreductase, a potential drug target. *Biochimica et Biophysica Acta (BBA) - Bioenergetics* **1859**, 191–200 (2018). doi: 10.1016/j.bbabio.2017.12.004

27. Narindrasorasak, S. *et al*. Characteristics and regulation of a phospholipid-activated malate oxidase from *Escherichia coli*. *Journal of Biological Chemistry* **254**, 1540–1545 (1979).

28. Kabashima, Y. *et al*. Purification and characterization of malate:quinone oxidoreductase from thermophilic *Bacillus* sp. PS3. *Journal of Bioenergetics and Biomembranes* **45**, 131–136 (2013). doi: 10.1007/s10863-012-9485-5

29. Rest, M. E. *et al*. Functions of the membrane-associated and cytoplasmic malate dehydrogenases in the citric acid cycle of *Escherichia coli*. *Journal of Bacteriology* **182**, 6892-6899 (2000). doi: 10.1128/jb.182.24.6892-6899.2000

30. Kretzschmar, U. *et al*. Malate:quinone oxidoreductase is essential for growth on ethanol or acetate in *Pseudomonas aeruginosa*. *Microbiology* **148**, 3839–3847 (2002). doi: 10.1099/00221287-148-12-3839

31. Molenaar, D. *et al*. Biochemical and genetic characterization of the membrane-associated malate dehydrogenase (acceptor) from *Corynebacterium glutamicum*. *European Journal of Biochemistry* **254**, 395–403 (1998). doi: 10.1046/j.1432-1327.1998.2540395.x

32. Asano, A., Kaneshiro, T. & Brodie, F. Malate-vitamin K reductase, a phospholipid-requiring enzyme., *Journal of Biological Chemistry* **240**, 895-905 (1965).

33. Mizuno, T. & Kageyama, M. Separation and Characterization of the Outer Membrane of *Pseudomonas aeruginosa*. *The Journal of Biochemistry* **84**, 179–191 (1978). doi: 10.1093/oxfordjournals.jbchem.a132106

34. Kather, B. *et al*. Another unusual type of citric acid cycle enzyme in *Helicobacter pylori*: the malate:quinone oxidoreductase. *Journal of Bacteriology* **182**, 3204–3209 (2000). doi: 10.1128/jb.182.11.3204-3209.2000

35. Molenaar, D. *et al*. Functions of the membrane-associated and cytoplasmic malate dehydrogenases in the citric acid cycle of *Corynebacterium glutamicum*. *Journal of Bacteriology* **182**, 6884–6891 (2000). doi: 10.1128/jb.182.24.6884-6891.2000

36. Francis, M. *et al*. The Oxidation of L-Malate by Pseudomonas sp . *Biochemical Journal* **84**, 430-438 (1963). doi:10.1042/bj0890430

37. Kimura, T. & Tobari, J. Participation of flavin-adenine dinucleotide in the activity of malate dehydrogenase from *Mycobacterium avium*. *Biochimica et Biophysica Acta* **73**, 399–405 (1963). doi: 10.1016/0006-3002(63)90441-4

38. Zaitseva, J. *et al*. Structure of *Escherichia coli* malate dehydrogenase at 1.45 Å resolution. *Acta Crystallographica Section F Structural Biology and Crystallization Communications* **65**, 866–869 (2009). doi: 10.1107/s1744309109032217

39. Wynne, S. A. *et al*. Tetrameric malate dehydrogenase from a thermophilic *Bacillus*: cloning, sequence and overexpression of the gene encoding the enzyme and isolation and characterization of the recombinant enzyme. *Biochemical Journal* **245**, 235–245 (1996). doi: 10.1042/bj3170235

40. Genda, T., Nakamatsu, T. & Ozak, H. Purification and characterization of malate dehydrogenase from *Corynebacterium glutamicum*. *Journal of Bioscience and Bioengineering* **95**, 562–566 (2003). Doi: 10.1263/jbb.95.562

41. Garvie, E. I. Bacterial lactate dehydrogenases. *Microbiology Reviews* **44**, 106–139 (1980).

42. Jiang, T. *et al*. Microbial lactate utilization: Enzymes, pathogenesis, and regulation. *Trends in Microbiology* **22**, 589–599 (2014). doi: 10.1016/j.tim.2014.05.008

43. Gao, C. *et al*. NAD-Independent *L*-Lactate Dehydrogenase Is Required for *L*-Lactate Utilization in *Pseudomonas stutzeri* SDM. *PLoS ONE* **7**, (2012). doi: 10.1371/journal.pone.0036519

44. Futai, M. & Kimura, H. Membrane *D*-lactate dehydrogenase from *Escherichia coli*. Purification and properties. *Biochemistry* **12**, 2468–2474 (1973).

45. Gao, C. *et al*. NAD-independent *L*-lactate dehydrogenase required for *L*-lactate utilization in *Pseudomonas stutzeri* A1501. *Journal of Bacteriology* **197**, 2239–2247 (2015).

46. Dym, O. *et al*. The crystal structure of *D*-lactate dehydrogenase, a peripheral membrane respiratory enzyme. *Proceedings of the National Academy of Sciences* **97**, 9413–9418 (2000). doi: 10.1073/pnas.97.17.9413

47. Jiang, T. *et al*. A bacterial multidomain NAD-independent *D*-lactate dehydrogenase utilizes flavin adenine dinucleotide and Fe-S clusters as cofactors and quinone as an electron acceptor for *D*-lactate oxidization. *Journal of Bacteriology* **199**, (2017). doi: 10.1128/jb.00342-17

48. Jasso-Chávez, R. *et al*. The bacterial-like lactate shuttle components from heterotrophic *Euglena gracilis*. *Biochimica et Biophysica Acta (BBA) - Bioenergetics* **1709**, 181–190 (2005). doi: 10.1016/j.bbabio.2005.07.007

49. Grace, D., Fetsch, A. & Karten, B. *Staphylococcus aureus*-A Foodborne Pathogen: Epidemiology, detection, characterization, prevention, and Control: An Overview; Pathogenesis of *Staphylococcus aureus*. in *Staphylococcus aureus* 3-5; 13-17 (Academic Press, 2018). doi:10.1128/AAC.50.4.1183

50. Watkins, R. R., David, M. Z. & Salata, R. A. Current concepts on the virulence mechanisms of meticillin-resistant *Staphylococcus aureus*. *Journal of Medical Microbiology* **61**, 1179–1193 (2012). doi: 10.1099/jmm.0.043513-0

51. Tavares, A. *et al*. High prevalence of hospital-associated methicillin-resistant *Staphylococcus aureus* in the community in Portugal: Evidence for the blurring of community-hospital boundaries. *European Journal of Clinical Microbiology & Infectious Diseases* **32**, 1269–1283 (2013). doi: 10.1007/s10096-013-1872-2

52. Nguyen, D. B. *et al*. Invasive methicillin-resistant *Staphylococcus aureus* infections among patients on chronic dialysis in the United States, 2005-2011. *Clinical Infectious Diseases* 57, 1393–1400 (2013). doi: 10.1093/cid/cit546

53. Hogg, S. Microbial Metabolism. in *Essential Microbiology* 109–154 (Wiley, 2005).

54. Sunderkötter, C. & Becker, K. Frequent bacterial skin and soft tissue infections: diagnostic signs and treatment. *JDDG: Journal der Deutschen Dermatologischen Gesellschaft* **13**, 501–526 (2015). doi: 10.1111/ddg.12721

55. Bukowski, M., Wladyka, B. & Dubin, G. Exfoliative toxins of *Staphylococcus aureus*. *Toxins* **2**, 1148–1165 (2010). doi: 10.3390/toxins2051148

56. Spaulding, A. R. *et al*. Staphylococcal and streptococcal superantigen exotoxins. *Clinical Microbiology Reviews* **26**, 422–447 (2013). doi: 10.1128/CMR.00104-12

57. Ferreira, M. T. *et al*. Effect of oxygen on glucose metabolism: utilization of lactate in *Staphylococcus aureus* as revealed by *in vivo* NMR studies. *PLoS One* ***8***, (2013). doi: 10.1371/journal.pone.0058277

58. Fuchs, S. *et al*. Anaerobic gene expression in *Staphylococcus aureus*. *Journal of Bacteriology* **189**, 4275–4289 (2007). doi: 10.1128/jb.00081-07

59. Dassy, B. & Fournier, J. M. Respiratory activity is essential for post-exponential-phase production of type 5 capsular polysaccharide by *Staphylococcus aureus*. *Infection and Immunity* **64**, 2408–14 (1996).

60. Becker, K., Heilmann, C. & Peters, G. Coagulase-negative staphylococci. *Clinical Microbiology Reviews* **27**, 870–926 (2014). doi: 10.1128/cmr.00109-13

61. Strasters, K. & Winkler, K. Carbohydrate Metabolism of *Staphylococcus aureus*. *Journal of General Microbiology* **33**, 213–229 (1963). doi: 10.1099/00221287-33-2-213

62. Somerville, G. A. *Staphylococcus aureus* metabolism and physiology. in *Staphylococcus*: genetics and physiology 107–118 (Caister Academic Press, 2016).

63. Diep, B. A. *et al*. Complete genome sequence of USA300, an epidemic clone of community-acquired meticillin-resistant *Staphylococcus aureus*. *The Lancet* **367**, 731–739 (2006). doi: 10.1016/s0140-6736(06)68231-7

64. Artzatbanov, V. Y. & Petrov, V. V. Branched respiratory chain in aerobically grown *Staphylococcus aureus* -oxidation of ethanol by cells and protoplasts. *Archives of Microbiology* **153**, 580–584 (1990). doi: 10.1007/bf00245268

65. Taber, H. W. & Morrison, M. Electron transport in staphylococci. Properties of a particle preparation from exponential phase *Staphylococcus aureus*. *Archives of Biochemistry and Biophysics* **105**, 367–379 (1964). doi: 10.1016/0003-9861(64)90021-9

66. Faller, A. & Schleifer, K. H. Modified oxidase and benzidine tests for separation of staphylococci from micrococci. *Journal of Clinical Microbiology* **13**, 1031–1035 (1981).

67. Faller, A. H., Götz, F. & Schleifer, K.-H. Cytochrome-patterns of Staphylococci and Micrococci and their taxonomic implications. *Zentralblatt für Bakteriol. I. Abt. Orig. C Allg. Angew. und ökologische Mikrobiol* **1**, 26–39 (1980). doi: 10.1016/s0172-5564(80)80014-5

68. Clements, M. O. *et. al.* CtaA of *Staphylococcus aureus* is required for starvation survival, recovery, and cytochrome biosynthesis. *Journal of Bacteriology* **181**, 501–507 (1999).

69. Hammer, N. D. *et al*. Two heme-dependent terminal oxidases power *Staphylococcus aureus* organ-specific colonization of the vertebrate host. *mBio* **4,** (2013). doi: 10.1128/mbio.00241-13

70. Cotter, P. A., Melville, S. B., Albrecht, J. A. & Gunsalus, R. P. Aerobic regulation of cytochrome d oxidase (cydAB) operon expression in *Escherichia coli*: roles of Fnr and ArcA in repression and activation. Mol. Microbiol. 25, 605–15 (1997).

71. Götz, F. & Mayer, S. Both terminal oxidases contribute to fitness and virulence during organ-specific *Staphylococcus aureus* colonization. MBio 4, 4–6 (2013). doi: 10.1128/mBio.00976-13

72. Rosário, A. L. *et al*. Expression, purification, crystallization and preliminary X-ray diffraction analysis of a type II NADH:quinone oxidoreductase from the human pathogen *Staphylococcus aureus*. *Acta Crystallographica Section F Structural Biology Communications* **71**, 477–482 (2015). doi: 10.1107/s2053230x15005178

73. Sena, F. V. *et al*. Type-II NADH: Quinone oxidoreductase from *Staphylococcus aureus* has two distinct binding sites and is rate limited by quinone reduction. *Molecular Microbiology* **98**, 272–288 (2015). doi: 10.1111/mmi.13120

74. Richter, D., Tiedge, H. & Vignais, P. Hydrogenases and Complex I. in *Bioenergetics* 45, 236–244 (2008).

75. Schurig-Briccio, L. A. *et al*. Characterization of the type 2 NADH:menaquinone oxidoreductases from *Staphylococcus aureus* and the bactericidal action of phenothiazines. *Biochimica et Biophysica Acta (BBA) - Bioenergetics* **1837**, 954–963 (2014).

76. Mayer, S. *et al*. The *Staphylococcus aureus* NuoL-like protein MpsA contributes to the generation of membrane potential. *Journal of Bacteriology* **197**, 794–806 (2015). doi: 10.1128/jb.02127-14

77. Fuller, J. R. *et al*. Identification of a lactate-quinone oxidoreductase in *Staphylococcus aureus* that is essential for virulence. *Frontiers in Cellular and Infection Microbiology* **1**, (2011). doi: 10.3389/fcimb.2011.00019

78. Zhang, X. *et al*. *Staphylococcus aureus* CidC is a pyruvate:menaquinone oxidoreductase. *Biochemistry* **56**, 4819–4829 (2017). doi: 10.1021/acs.biochem.7b00570

79. Gaupp, R. *et al*. Advantage of upregulation of succinate dehydrogenase in S*taphylococcus aureus* biofilms. *Journal of Bacteriology* **192**, 2385–2394 (2010). doi: 10.1128/jb.01472-09

80. Spahich, N. A. *et al*. *Staphylococcus aureus* lactate- and malate-quinone oxidoreductases contribute to nitric oxide resistance and virulence. *Molecular Microbiology* **100**, 759–773 (2016). doi: 10.1111/mmi.13347

81. Marreiros, B. C. *et al*. A missing link between complex I and group 4 membrane-bound [NiFe] hydrogenases. *Biochimica et Biophysica Acta (BBA) - Bioenergetics* 1827, 198–209 (2013). doi: 10.1016/j.bbabio.2012.09.012

82. Stockland, A. E. & Clemente, C. L. S. Multiple forms of lactate dehydrogenase in *Staphylococcus aureus* multiple forms of lactate dehydrogenase. *Journal of Bacteriology* **100** 347–353 (1969).

83. Inoue, H., Nojima, H. & Okayama, H. High efficiency transformation *of Escherichia coli* with plasmid. *Gene* **96**, 23–28 (1990). doi: 10.1016/0378-1119(90)90336-p

84. Kubicek, J. *et al*. Expression and purification of membrane proteins. *Methods in Enzymology Laboratory Methods in Enzymology: Protein Part C* **541**, 117–140 (2014). doi: 10.1016/b978-0-12-420119-4.00010-0

85. Schlegel, S. *et al*. Optimizing Membrane Protein Overexpression in the *Escherichia coli* strain Lemo21(DE3). *Journal of Molecular Biology* **423**, 648–659 (2012). doi: 10.1016/j.jmb.2012.07.019

86. Fotiadis, D., Harder, D. & Fotiadis. Preparation of detergent-solubilized membranes from *Escherichia coli*. *Protocol Exchange* (2012). doi: 10.1038/protex.2012.033

87. Watters, C. A one-step biuret assay for protein in the presence of detergent. *Analytical Biochemistry* **88**, 695–698 (1978). doi: 10.1016/0003-2697(78)90475-x

88. Grabski, A. C. & Burgess, R. R. Preparation of protein samples for SDS-polyacrylamide gel electrophoresis: procedures and tips. *Innovations* **13**, 10–12 (2001).

89. Haegerhaell, C. *et al*. Two hemes in *Bacillus subtilis* succinate:menaquinone oxidoreductase (Complex II). *Biochemistry* **31**, 7411–7421 (1992). doi: 10.1021/bi00147a028

90. Kozioł, J. [132] Fluorometric analyses of riboflavin and its coenzymes. *Vitamins and Coenzymes Methods in Enzymology* 253–285 (1971). doi: 10.1016/s0076-6879(71)18089-5

91. Vitko, N. & Richardson, A. Laboratory Maintenance of Methicillin-Resistant *Staphylococcus aureus* (MRSA). *Current Protocols in Microbiology*, (2013). doi: 10.1002/9780471729259.mc09c02s28

92. Pattee, P. A. & Neveln, D. S. Transformation analysis of three linkage groups in *Staphylococcus aureus*. *Journal of Bacteriology* **124**, 201–211 (1975).

93. Hussain, M., Hastings, J. G. M. & White, P. J. A chemically defined medium for slime production by coagulase-negative staphylococci. Journal of Medical Microbiology 34, 143–147 (1991). doi: 10.1099/00222615-34-3-143

94. Nair, D. R. *et al.* Characterization of a novel small molecule that potentiates *β*-lactam activity against gram-positive and gram-negative pathogens. *Antimicrobial Agents and Chemotherapy* **59**, 1876–1885 (2015). doi: 10.1128/aac.04164-14

95. Wagner, S. *et al*. Tuning *Escherichia coli* for membrane protein overexpression. *Proceedings of the National Academy of Sciences* **105**, 14371–14376 (2008). doi: 10.1073/pnas.0804090105

96. Thauer, R. K., Jungermann, K. & Decker, K. Energy conservation in chemotrophic anaerobic bacteria. *Microbial and Molecular Biology Reviews* **41**, 100–180 (1977).

97. Itagaki, E. & Hager, P. L. Studies on Cytochrome b_{562} of *Escherichia coli*. I. Purification and crystallization of cytochrome b_{562}. *Journal of Biological Chemistry* **241**, 3687–3695 (1966).

98. Giacometti, J. & Josić, D. Protein and Peptide Separations. in *Liquid Chromatography* 149–184 (Elsevier, 2013). doi:10.1016/b978-0-12-415806-1.00007-3

99. Hage, D. S. *et al*. Affinity Chromatography. in *Liquid Chromatography* 1–23 (Elsevier, 2013). doi:10.1016/b978-0-12-415806-1.00001-2

100. Futai, M & Kimura H. Inducible membrane-bound *L*- lactate dehydrogenase from *Escherichia coli*. Purification and properties. *Journal of Biological Chemistry* **252**, 5820-5827 (1977)

101. García-Angulo, V. A. Overlapping riboflavin supply pathways in bacteria. *Critical Reviews in Microbiology* **43**, 196–209 (2017). doi: 10.1080/1040841x.2016.1192578.

102. Bosi, E. *et al*. Comparative genome-scale modelling of *Staphylococcus aureus* strains identifies strain-specific metabolic capabilities linked to pathogenicity. *Proceedings of the National Academy of Sciences* **113**, (2016). doi: 10.1073/pnas.1523199113

103. Zhang, P., Wang, J. & Shi, Y. Structure and mechanism of the S component of a bacterial ECF transporter. *Nature* **468**, 717–720 (2010). doi: 10.1038/nature09488

104. Jaehme, M. & Slotboom, D. J. Diversity of membrane transport proteins for vitamins in bacteria and archaea. *Biochimica et Biophysica Acta (BBA) - General Subjects* **1850**, 565–576 (2015). doi: 10.1016/j.bbagen.2014.05.006

105. Halsey, C. R. *et al*. Amino acid catabolism in *Staphylococcus aureus* and the function of carbon catabolite repression. *mBio* **8**, (2017). doi: 10.1128/mBio.01434-16

106. Blumenthal, H. J., Huettner, C. F. & Montiel, F. A. Comparative aspects of glucose catabolism in *Staphylococcus aureus* and *S. epidermidis*. *Annals of the New York Academy of Sciences* **236**, 105–114 (1974). doi: 10.1111/j.1749-6632.1974.tb41485.x

107. Seidl, K. *et al*. *Staphylococcus aureus* CcpA Affects Virulence Determinant Production and Antibiotic Resistance. *Antimicrobial Agents and Chemotherapy* **50**, 1183–1194 (2006). doi: 10.1128/AAC.50.4.1183-1194.2006

108. Zhu, Y. *et al.* Tricarboxylic acid cycle-dependent attenuation of *Staphylococcus aureus in vivo* virulence by selective inhibition of amino acid transport. *Infection and Immunity* **77**, 4256–4264 (2009). doi: 10.1128/IAI.00195-09

109. Goldschmidt, M. C. & Powelson, D. M. Effect of the culture medium on the oxidation of acetate by *Micrococcus pyogenes* var. *aureus*. *Archives of Biochemistry and Biophysics* **46**, 154–163 (1953).

110. Somerville, G. A. *et al*. Synthesis and deformylation of *Staphylococcus aureus* delta-toxin are linked to tricarboxylic acid cycle activity. *Journal of Bacteriology* **185**, 6686–6694 (2003). doi: 10.1128/jb.185.22.6686-6694.2003

111. Ledala, N. *et al*. Influence of iron and aeration on *Staphylococcus aureus* growth, metabolism, and transcription *Journal of Bacteriology* **196**, 2178–2189 (2014). doi: 10.1128/JB.01475-14

112. Somerville, G. A. & Proctor, R. A. The Biology of Staphylococci. in *Staphylococci in Human Disease* 53, 3–17 (Wiley/Blackwell, 2010).

113. Chalovich, J. M. & Eisenberg, E. NMR Analysis of a stress response metabolic signalling network. *Journal of Proteome Research* **10**, 3743-3754 (2011). doi: 10.1021/pr200360w

114. Gaupp, R. *et al*. *Staphylococcus aureus* metabolic adaptations during the transition from a daptomycin susceptibility phenotype to a daptomycin nonsusceptibility phenotype. *Antimicrobial Agents and Chemotherapy* **59**, 4226–4238 (2015). doi: 10.1128/aac.00160-15

115. Nelson, J. L. *et al*. Vancomycin-intermediate *Staphylococcus aureus* strains have impaired acetate catabolism: Implications for polysaccharide intercellular adhesin synthesis and autolysis. *Antimicrobial Agents and Chemotherapy* **51**, 616–622 (2006). doi: 10.1128/aac.01057-06

116. Dörries, K. & Lalk, M. Metabolic footprint analysis uncovers strain specific overflow metabolism and *D*-isoleucine production of *Staphylococcus aureus* COL and HG001. *PLoS One* **8**, (2013). doi: 10.1371/journal.pone.0081500

117. Gardner, J. F. & Lascelles, J. The requirement for acetate of a streptomycin-resistant strain of *Staphylococcus aureus*. *Journal of General Microbiology* **29**, 157–164 (1962). doi: 10.1099/00221287-29-1-157

118. Liebeke, M. et al. A metabolomics and proteomics study of the adaptation of *Staphylococcus aureus* to glucose starvation. *Molecular BioSystems* **7**, 1241–1253 (2011). doi: 10.1039/c0mb00315h

119. Somerville, G. A. *et al*. *Staphylococcus aureus* aconitase inactivation unexpectedly inhibits post-exponential-phase growth and enhances stationary-phase survival. *Infection and Immunity* **70**, 6373–6382 (2002). doi: 10.1128/IAI.70.11.6373-6382.2002

120. Liew, A. T. F. *et al*. A simple plasmid-based system that allows rapid generation of tightly controlled gene expression in *Staphylococcus aureus*. *Microbiology* **157** Pt3, 666–676 (2017). doi:10.1099/mic.0.045146-0

Website Bibliography

WHO European Health Information (2017, November 17) At Your Fingertips. Retrieved 2018,May 28, from https://gateway.euro.who.int/en/indicators/amr_23-methicillin-resistant-staphylococcus-aureus-mrsa/

7. Supporting Information

7.1 Medium composition

This section describes all the medium compositions used to performed bacterial growths. Table S1 describes the medium used for *E. coli* growths and Table S2 and S3 describe the ones used for *S. aureus* growth.

Table S1- **Medium composition used for *E. coli* growths**

		Medium			
Reagent Supplier	Ingredients	LB	SOB	2x YT	TB
Pancreac	Tryptone	10 g/L	20 g/L	16 g/L	20 g/L
Fisher	Yeast extract	5 g/L	5 g/L	10 g/L	24 g/L
Thermo Scientific	Sodium chloride	10 g/L	0.5 g/L	5 g/L	
Panreac	Potassium chloride		0.0186 g/L		
Pancreac/ Pancreac	Solution of potassium dihydrogen phosphate/ dipotassium hydrogen phosphate trihydrate				0.017 M
Fisher Scientific	Glycerol				4 mL/L

Table S2- **Medium composition used for *S. aureus* growths**

		Medium
Reagent Supplier	Ingredients	TSA
BD biosciences	Casein peptone	15 g/L
Roth	Soya peptone	5 g/L
Thermo Scientific	Sodium chloride	5 g/L
Fragon	Agar	15 g/L

Preparation of CDM was based on the work of Vitko et. *al l* [91], Patte et. *al* [92] and Hussain et. *al* [93].
The components of the medium were first made separately in 5 groups. All groups were made as concentrated solutions as follows: group 1, x10; group 2 and 3, x100; group 4 and 5; x1000. Except for group 1, the components of each group were mixed, the final volume adjusted and the solution was filtered. Group 4 included a riboflavin stock. The ingredients of group 1 were mixed and the solution volume adjusted to 1000 mL with distilled water and autoclaved at 121 °C for 15 min. Group 2 and 3 components were prepared and stored separately to maximize the storage longevity.
All the solutions present in Table S3 were stored at 4 °C. To make 100 mL of medium it is needed to add 10 mLs of group 1 solution, 1 mL of each component of group 2, group 3 and 0.1 mL of group 4 and group 5, followed by the addition of the desired carbon source. The pH is then adjusted to 7.4 using 10 M NaOH, brought to the desired volume using ddH_2O and then filter sterilized.

Table S3- **CDM medium composition**

Reagent Supplier	Ingredient	Amount (g/L)	Solvent	Reagent Supplier	Ingredient	Amount (g/L)	Solvent
	Group 1 (Salt Solution)				**Group 3 (Nitrogenous Bases)**		
Panreac	K_2HPO_4	70	dH_2O	Sigma Aldrich	Adenine	0.5	
	KH_2PO_4	20		Alfa Aesar	Cytosine	0.5	
	$(NH_4)_2SO_4$	10		Sigma Aldrich	Guanine	0.5	dH_2O
Merck	$MgSO_4.7H_2O$	0.5		Alfa Aesar	Thymine	2	
				Sigma Aldrich	Uracil	0.5	
	Group 2 (Amino Acid)				**Group 4 (Vitamin Solution)**		
	L-Phenylalanine	4	1 M NH_4OH	Alfa Aesar	Thiamine	1	
	L-Isoleucine	3			Niacin	1.2	dH_2O
	L-Tyrosine	5		Sigma Aldrich	Biotin	5E-3	
	Cystine	2			Ca Pantothenate	0.25	
	L-Glutamate	10			Riboflavin	1.2	
	L-Lysine	1			**Group 5 (Trace elements)**		
Sigma Aldrich	*L*-Methionine	7	1 M HCl	VWR	$FeCl_3$	8	
	L-Histidine	3		Merck	ZnCl	0.07	
	L-Tryptophan	1			$MnCl.4H_2O$	1	
	L-Leucine	9		Sigma Aldrich	Boric Acid	6E-3	dH_2O
	L-Aspartate	9		Pancrec	$CoCl_2.6H_2O$	0.397	
	L-Arginine	7			$CuCl_2.2H_2O$	2.56E-3	
	L-Serine	3		Merck	$NiCl_2.6H_2O$	0.0238	
	L-Alanine	6			$Na_2MoO_4.2H_2O$	0.0358	
	L-Threonine	3	dH_2O				
Roth	*L*-Glycine	5					
Sigma Aldrish	*L*-Valine	8					
Merck	*L*-Proline	1					

7.2 Complementary Information

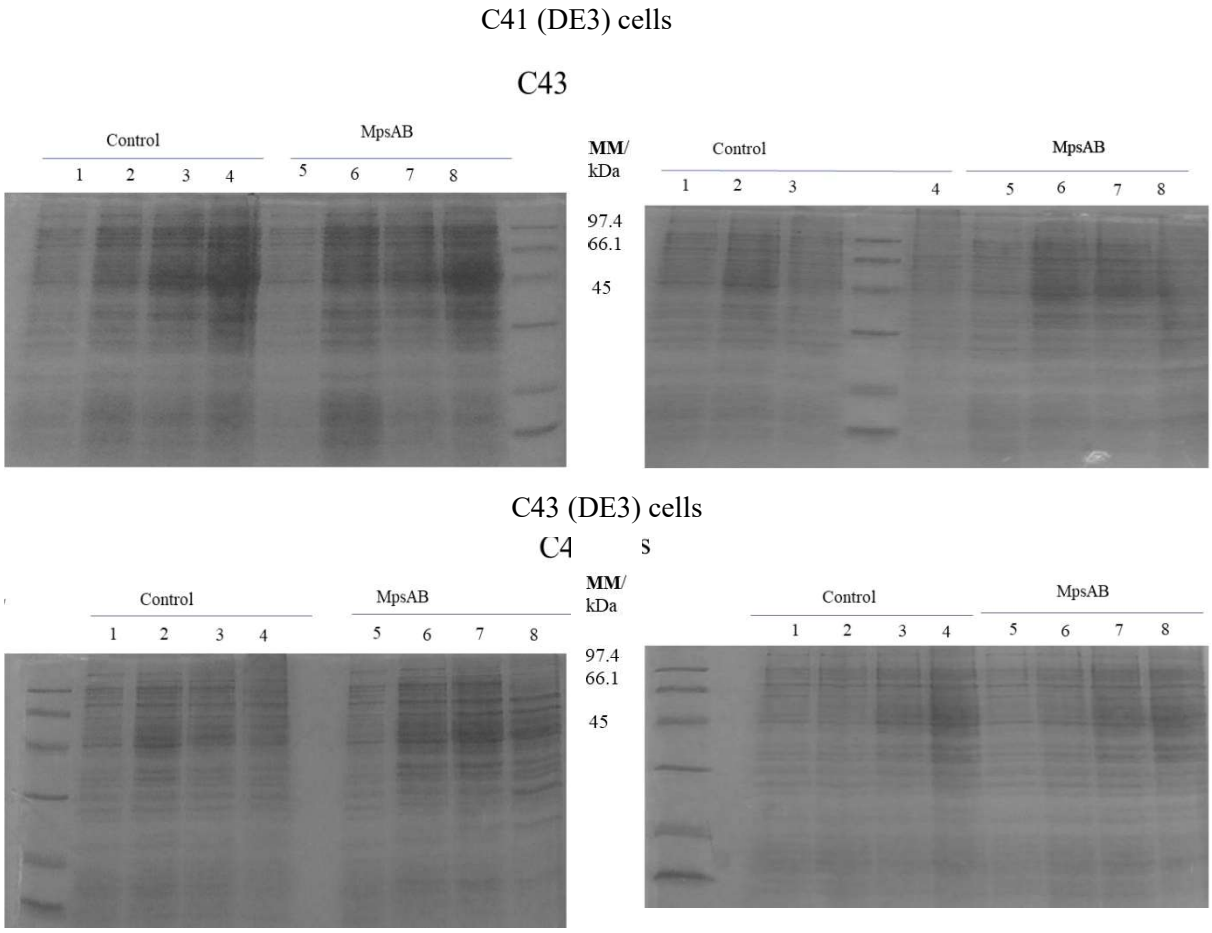

Figure S1- **Expression test made with C41 (DE3) and C43 (DE3) cells.** 15 % Acrylamide SDS-PAGE. In all acrylamide gel lanes 1-4 represent the protein induction of the pET21(+)b control plasmid while lanes 5-8 represent protein induction of the pET21(+)b-MpsAB-6xHisTag.Lane 1 and 5; before protein expression induction; Lane 2 and 6; 2 hours after protein induction; Lane 3 and 7; 4 hours after protein induction; lane 4 and 8, 6 hours after protein induction. Lane M, Protein marker Low-Range (BioRad)

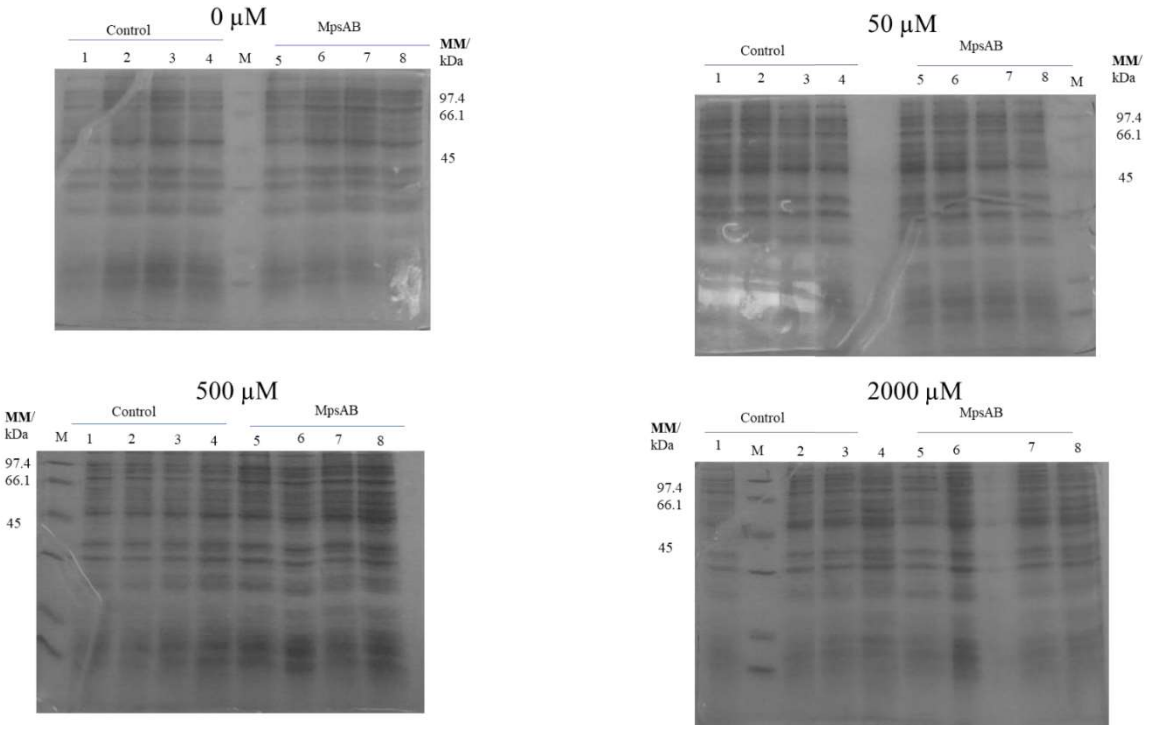

Figure S2- **Expression test made with Lemo21(DE3) testing different *L*-rhamnose concentrations.** 15 % Acrylamide SDS-PAGE. In all acrylamide gels lane 1-4 represent protein induction of the control plasmid pET21(+)b while the other lanes 5-8 represent the protein complex expression when the plasmid pET21(+)b-MpsAB-6xHisTag was transformed. Lane 1 and 5; before protein expression induction; Lane 2 and 6; 2 hours after protein induction; Lane 3 and 7; 4 hours after protein induction; lane 4 and 8, 6 hours after protein induction. Lane M, Protein marker Low-Range (BioRad)

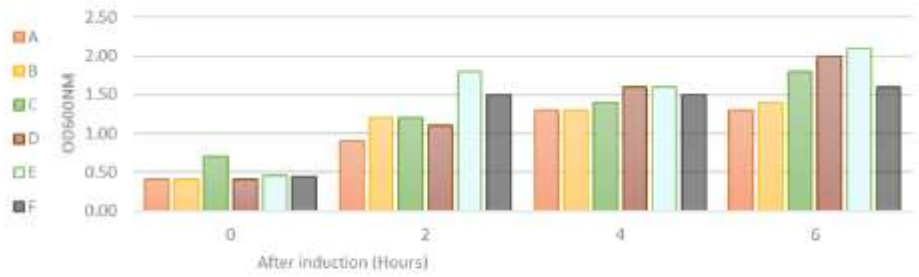

Figure S3- **Comparison of OD_{600nm} reached by the expression tests using LEMO21(DE3) with no *L*-rhamnose.** Each condition is represented by a letter that corresponds to the condition described in table 4.1

A

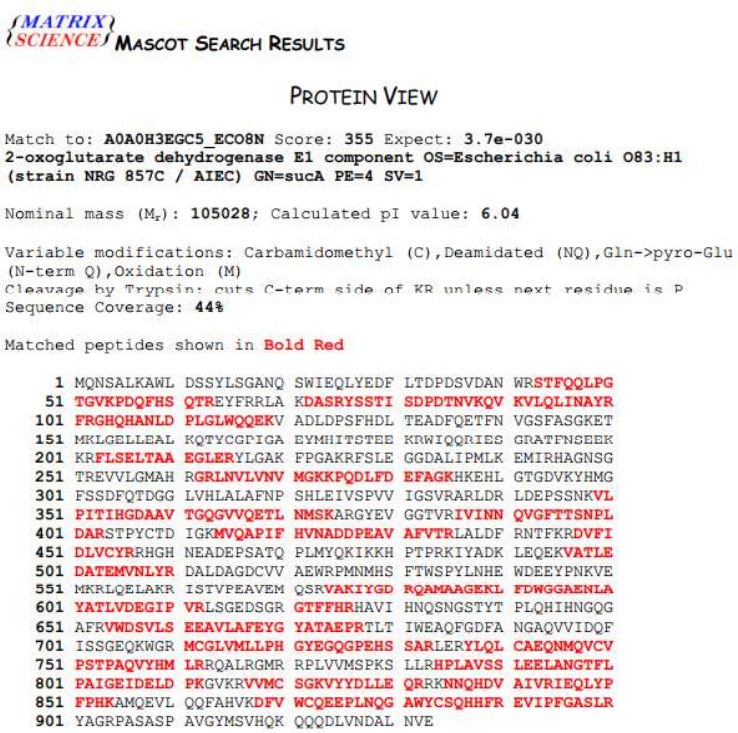

MASCOT SEARCH RESULTS

PROTEIN VIEW

Match to: **A0A0H3EGC5_ECO8N** Score: **355** Expect: **3.7e-030**
2-oxoglutarate dehydrogenase E1 component OS=Escherichia coli O83:H1 (strain NRG 857C / AIEC) GN=sucA PE=4 SV=1

Nominal mass (M_r): **105028**; Calculated pI value: **6.04**

Variable modifications: Carbamidomethyl (C),Deamidated (NQ),Gln->pyro-Glu (N-term Q),Oxidation (M)
Cleavage by Trypsin: cuts C-term side of KR unless next residue is P
Sequence Coverage: **44%**

Matched peptides shown in **Bold Red**

```
     1 MQNSALKAWL DSSYLSGANQ SWIEQLYEDF LTDPDSVDAN WRSTFQQLPG
    51 TGVKPDQFHS QTREYFRRLA KDASRYSSTI SDPDTNVKQV KVLQLINAYR
   101 FRGHQHANLD PLGLWQQEKV ADLDPSFHDL TEADFQETFN VGSFASGKET
   151 MKLGELLEAL KQTVCGPIGA EYMHITSTEE KRWIQQRIES GRATFNSEEK
   201 KRFLSELTAA EGLERYLGAK FPGAKRFSLE GGDALIPMLK EMIRHAGNSG
   251 TREVVLGMAH RGRLNVLVNV MGKKPQDLFD EFAGKHKEHL GTGDVKYHMG
   301 FSSDFQTDGG LVHLALAFNP SHLEIVSPVV IGSVRARLDR LDEPSSNKVL
   351 PITIHGDAAV TGQGVVQETL NMSKARGYEV GGTVRIVINN QVGFTTSNPL
   401 DARSTPYCTD IGKMVQAPIF HVNADDPEAV AFVTRLALDF RNTFKRDVFI
   451 DLVCYRRHGH NEADEPSATQ PLMYQKIKKH PTPRKIYADK LEQEKVATLE
   501 DATEMVNLYR DALDAGDCVV AEWRPMNMHS FTWSPYLNHE WDEEYPNKVE
   551 MKRLQELAKR ISTVPEAVEM QSRVAKIYGD RQAMAAGEKL FDWGGAENLA
   601 YATLVDEGIP VRLSGEDSGR GTFFHRHAVI HNQSNGSTYT PLQHIHNGQG
   651 AFRVWDSVLS EEAVLAFEYG YATAEPRTLT IWEAQFGDFA NGAQVVIDQF
   701 ISSGEQKWGR MCGLVMLLPH GYEGQGPEHS SARLERYLQL CAEQNMQVCV
   751 PSTPAQVYHM LRRQALRGMR RPLVVMSPKS LLRHPLAVSS LEELANGTFL
   801 PAIGEIDELD PKGVKRVVMC SGKVYYDLLE QRRKNNQHDV AIVRIEQLYP
   851 FPHKAMQEVL QQFAHVKDFV WCQEEPLNQG AWYCSQHHFR EVIPFGASLR
   901 YAGRPASASP AVGYMSVHQK QQQDLVNDAL NVE
```

B

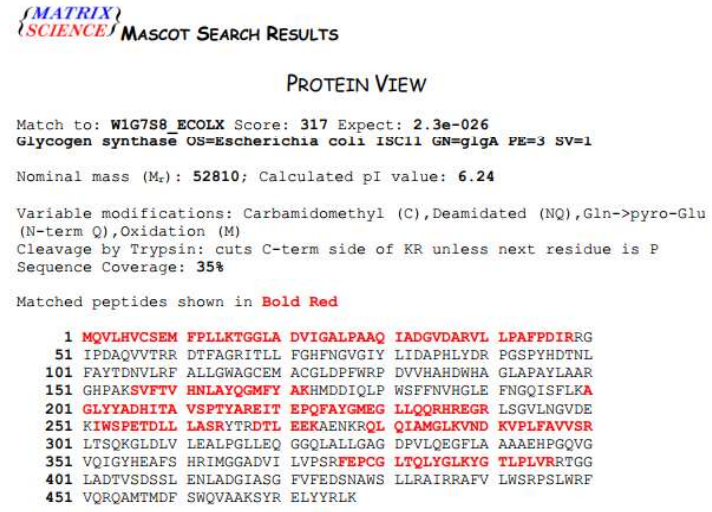

MASCOT SEARCH RESULTS

PROTEIN VIEW

Match to: **W1G7S8_ECOLX** Score: **317** Expect: **2.3e-026**
Glycogen synthase OS=Escherichia coli ISC11 GN=glgA PE=3 SV=1

Nominal mass (M_r): **52810**; Calculated pI value: **6.24**

Variable modifications: Carbamidomethyl (C),Deamidated (NQ),Gln->pyro-Glu (N-term Q),Oxidation (M)
Cleavage by Trypsin: cuts C-term side of KR unless next residue is P
Sequence Coverage: **35%**

Matched peptides shown in **Bold Red**

```
     1 MQVLHVCSEM FPLLKTGGLA DVIGALPAAQ IADGVDARVL LPAFPDIRRG
    51 IPDAQVVTRR DTFAGRITLL FGHFNGVGIY LIDAPHLYDR PGSPYHDTNL
   101 FAYTDNVLRF ALLGWAGCEM ACGLDPFWRP DVVHAHDWHA GLAPAYLAAR
   151 GHPAKSVFTV HNLAYQGMFY AKHMDDIQLP WSFFNVHGLE FNGQISFLKA
   201 GLYYADHITA VSPTYAREIT EPQFAYGMEG LLQQRHREGR LSGVLNGVDE
   251 KIWSPETDLL LASRYTRDTL EEKAENKRQL QIAMGLKVND KVPLFAVVSR
   301 LTSQKGLDLV LEALPGLLEQ GGQLALLGAG DPVLQEGFLA AAAEHPGQVG
   351 VQIGYHEAFS HRIMGGADVI LVPSRFEPCG LTQLYGLKYG TLPLVRRTGG
   401 LADTVSDSSL ENLADGIASG FVFEDSNAWS LLRAIRRAFV LWSRPSLWRF
   451 VQRQAMTMDF SWQVAAKSYR ELYYRLK
```

Figure S4- **MS identification of the chosen bands of the SDS-PAGE from the purified fraction containing the MpsAB-6xHisTag** (A) identification of the band with higher mass (B) identification of the band with lower mass

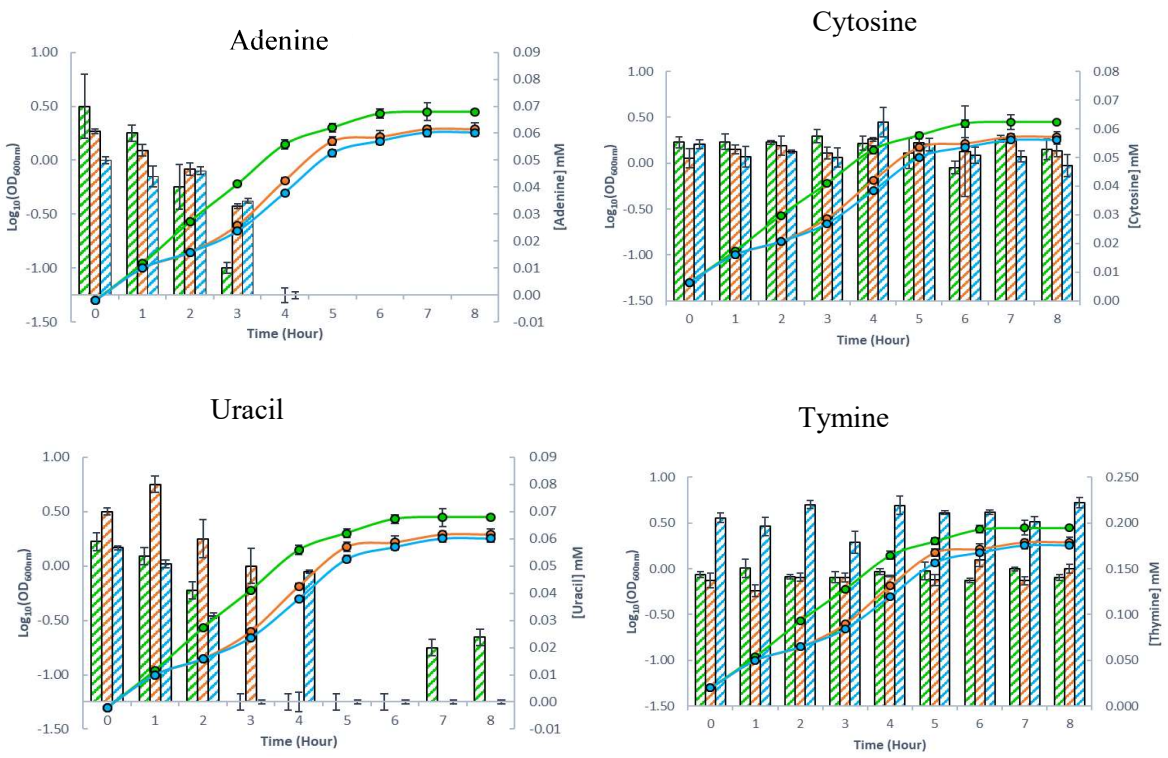

Figure S5 -**Nitrogenous base uptake pattern for the three strains.** Extracellular concentration of the identifiied nitrogenous bases for the MQOI::Tn strain (orange) and MQOII::Tn strain (Blue). The data represent are mean values ±SE values from three biological replicates.

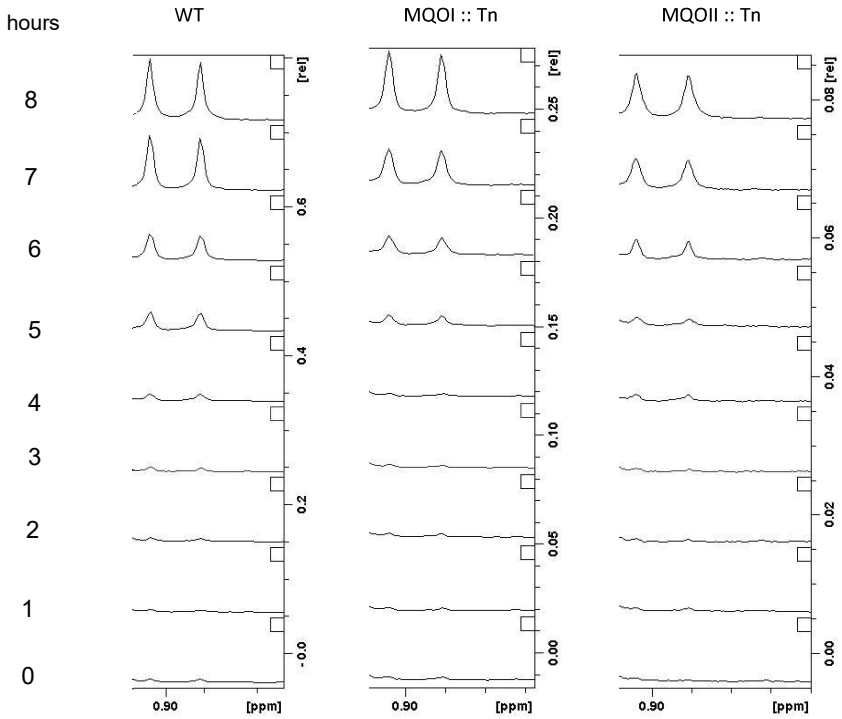

Figure S6- **Secretion of an unknown metabolite at 0.9 and 0.88 ppm.** Raw data from NMR spectra where it is shown the variation with time of the unknown metabolite for the three strains.

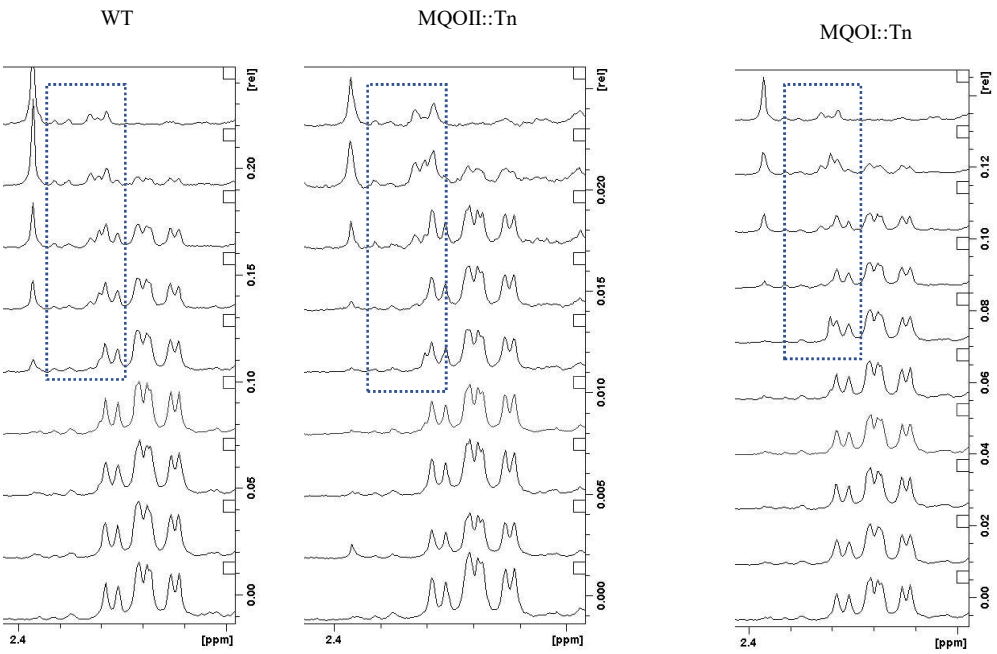

Figure S7- **Pyruvic acid Identification for the three strains.** Raw spectra where it is shown the variation with time for the spectra where the signals of glutamic acid and pyruvate appear. The blue square highlights the possible chemical shifts for pyruvate.

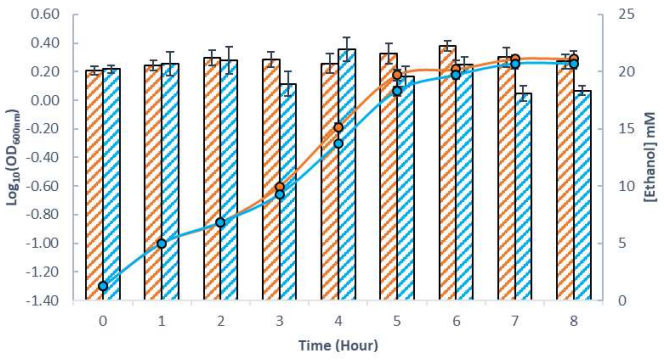

Figure S8-**Evaluation of ethanol concentration during the growth for the mutant strains.** Ethanol extracellular concentration for the MQOI::Tn strain (orange) and MQOII::Tn strain (Blue). The data represented are mean values ± SE values from three biological replicates.

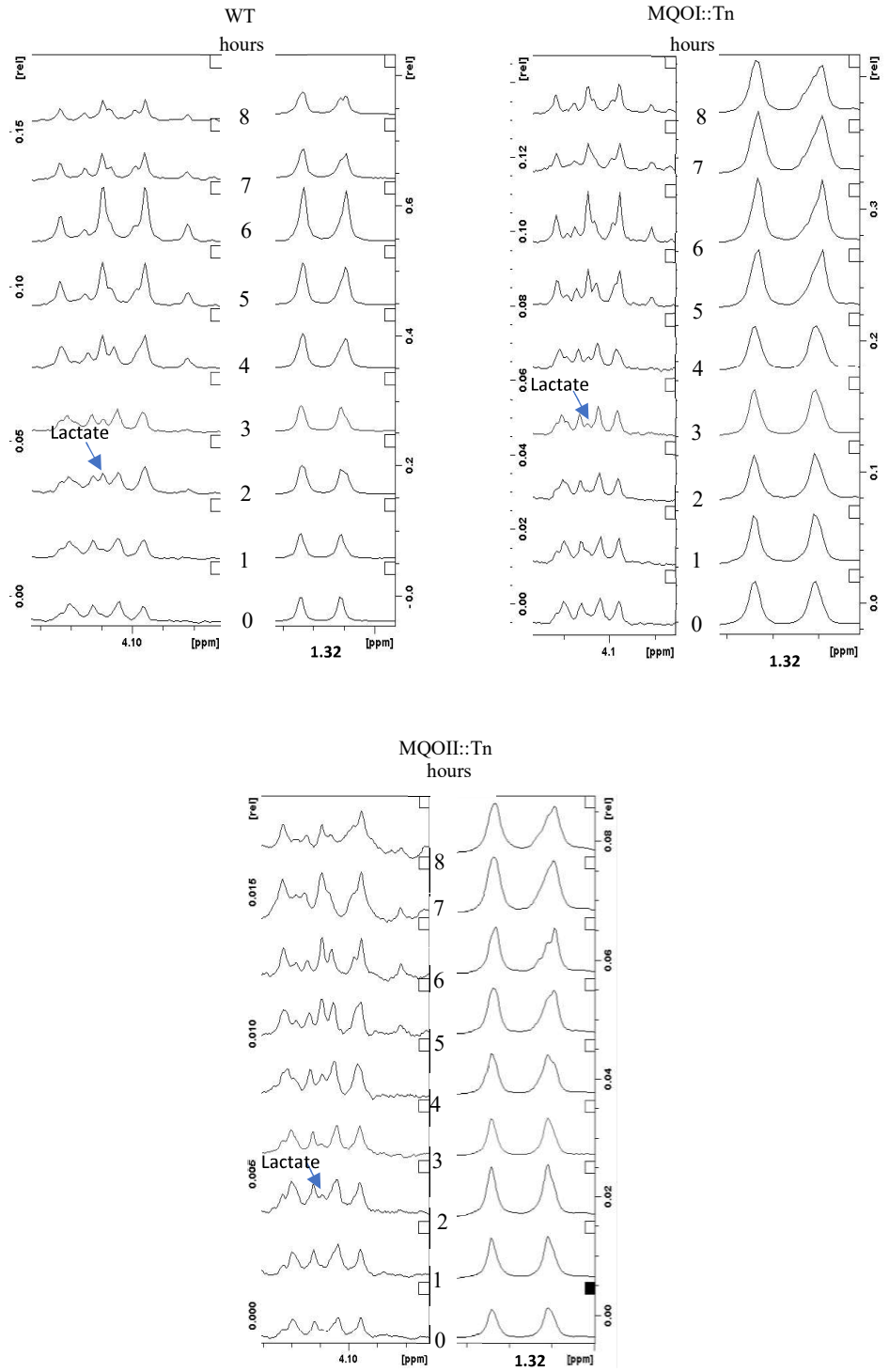

Figure S9- **Temporal evaluation of lactate.** Raw spectra where it shown the temporal variation for the chemical shifts of lactate. Blue arrows indicated when lactate appears.